FERRIMAGNETIC FLUORIDES

ALAIN TRESSAUD and JEAN MICHEL DANCE

Laboratoire de Chimie du Solide du C.N.R.S., Université de Bordeaux I, Talence, France

I. Introduction

Magnetic properties of matter have fascinated the human mind since antiquity. This particular interest has led men to create one of the most coherent frameworks of the theory of matter, which has evolved from the "divine force" invoked by Plato to modern quantum magnetodynamics.

At the same time the applications of magnetism have multiplied from the ancient nautical compass, which permitted the exploration of the world, to the giant modern computers, which allow the exploration of the cosmos.

The materials used have been for the most part oxides: hexagonal ferrites, spinels, orthoferrites, garnets, CrO_2. There are two reasons for this approach. First, it is natural for the technician to be interested in oxides because of the ease of preparation and manufacture, and second, the character of the transition element–oxygen bond, intermediate between pure ionic and pure covalent, makes the ferrimagnetic oxides insulators with Curie temperatures suitable for numerous applications. Nevertheless, the growing sophistication of electronic equipment requires the use of materials with more and more specific

properties. Therefore, the fluorides, which are very good electronic insulators because of the great electronegativity of fluorine and which often have higher transparency than the oxides in the visible region of the spectrum, have attracted the attention of researchers.

In addition to the practical interest for solid state physics in new transparent, strongly magnetic materials, the study of the magnetic properties of ferrimagnetic fluorides—on the basis of the semiempirical theories of Anderson, Goodenough, and Kanamori—gives a good idea of the nature of the magnetic interactions because of the greater simplicity of the bonding in fluorides as compared with oxides.

II. Magnetic Interactions in Insulators

Magnetic interactions in ferrimagnetic fluorides can be treated essentially on the basis of the exchange interactions theories. The results obtained from these theories can be correlated with the nature of the chemical bonding, thus giving valuable information to the solid state chemist. General articles on these subjects can be found in Anderson (*5*), Goodenough (*64*), Herpin (*80a*), Kittel (*91a*), Mabbs and Machin (*106a*), Owen and Thornley (*125*), and Rado and Suhl (*135a*).

A. The Exchange Integral

"Magnetically concentrated" materials can be distinguished from paramagnetic compounds by the presence of interactions between magnetic dipoles of neighboring magnetic atoms. The rules governing paramagnetism are based on the hypothesis of noninteraction between two spins of magnetic ions. Where two magnetic ions are close enough, a coupling between the moments of these two ions tends to align them along one direction. If the structure is three-dimensional in spite of the rapid decrease of this interaction with the distance, regions with spontaneous moments will appear in the case of ferri- or ferromagnetism and with canceled moments (nil spontaneous magnetization) for antiferromagnetism. Thermal agitation tends to weaken these couplings and H annihilate them at a critical temperature (T_C or T_N).

The presence of a spontaneous magnetization, which is incompatible with the results of the magnetism of "isolated" ions, can be explained phenomenologically by the Weiss molecular field, which is a hypothetical magnetic field representing the interaction of a given atom with all its magnetic neighbors. This field must be added to the applied field H_0, so that the effective field on the atom is

$$\mathbf{H}_{\text{eff}} = \mathbf{H}_0 + \mathbf{H}_{\text{mol}} \tag{1}$$

Weiss's hypothesis is that this molecular field $\mathbf{H}_{mol}$ is proportional to the average magnetization (features of Langevin's model can be noted here).

The quantal interpretation of ferromagnetism has been developed by Heisenberg and Dirac, who showed that the energy of interaction between two orbitals could be written with classic terms added to another term related to Pauli's principle and to the indistinguishability of electrons. This exchange energy is

$$E_J = \iint \varphi_a(\mathbf{r}_1)^* \varphi_b(\mathbf{r}_2)^* \frac{e^2}{|\mathbf{r}_1 - \mathbf{r}_2|} \varphi_a(\mathbf{r}_1)\varphi_b(\mathbf{r}_2)\, d\tau_1\, d\tau_2 \qquad (2)$$

where φ_a and φ_b are two wave functions corresponding to two different states for electrons 1 and 2, φ_a^* and φ_b^* their conjugated wave functions, and r_1 and r_2 the spatial distributions of the electrons. The origin of the exchange energy is electrostatic (e^2/r) and is one order of magnitude greater than the magnetic energy. In the case of ferromagnets, the spin alignment is due to Pauli's principle; the electrostatic energy is weaker when the spins are parallel, i.e., when the spin's wave function is completely symmetrical and the space function completely antisymmetrical. Because each spin is related to a net moment of $\boldsymbol{\mu} = 2\beta\mathbf{S}$, parallelism leads to a magnetic material.

Dirac transformed Heisenberg's energy formula into a spin Hamiltonian and generalized it to $\mathbf{S}_i$ and $\mathbf{S}_j$ interacting spins belonging to i and j atoms,

$$\mathscr{H} = -2 \sum_{i \le j} \sum_{j=1}^{J=N} J_{ij}(R_{ij}) \mathbf{S}_i \mathbf{S}_j \qquad (3)$$

(Heisenberg–Dirac–Van Vleck Hamiltonian) (*181*).

The exchange integral J_{ij} can only be evaluated experimentally. For an atom i having p electrons with a resultant $\mathbf{S}_i$,

$$\mathbf{S}_i = \sum_{k=1}^{p} \mathbf{S}_{i,k}$$

and, if the interatomic exchange integral is the same for the different electrons of the two atoms,

$$\begin{aligned} \mathscr{H}_{ij} &= -2 \sum_{k(i)} \sum_{l(i)} J_{ij} \mathbf{S}_k \cdot \mathbf{S}_l \\ &= -2J_{ij} \left(\sum_k \mathbf{S}_k \right) \cdot \left(\sum_l \mathbf{S}_l \right) \\ &= -2J_{ij} \mathbf{S}_i \mathbf{S}_j \end{aligned} \qquad (4)$$

Here J is an energy (identical with E_j) that falls off rapidly with the distance (R_{ij}) between 2 atoms, and only the interaction between the nearest neighbors is taken into account. It can be considered as the evaluation of the overlap of the electron charge distribution of 2 atoms.

According to the Heisenberg–Dirac theory, the exchange integral characterizing an interaction between 1 atom and its Z magnetic nearest neighbors with spins S is

$$|J| = \frac{3kT_c}{2ZS(S + 1)}$$

where k is the Boltzmann constant and T_c the magnetic transition temperature.

Many attempts to improve this calculation have been made (*43*, *143*, *161*). Among them, the Bethe–Peierls–Weiss method takes into account not only the interaction between 1 atom and its neighbors but also the interaction between the surrounding atoms (*24*, *189*). Smart (*155*, *156*) summarized the methods of calculation of exchange integrals in various structural types, using various experimental data: the transition point, the heat capacity, the susceptibility at the Néel point (in the case of antiferromagnets), etc.

The phenomenological theory of ferromagnetism using the Weiss molecular field concepts has been generalized by Néel (*119*) by giving either positive or negative values to the molecular field coefficients. This generalization has made it possible to explain most of the magnetic properties of antiferro- and ferrimagnetic compounds. The mechanism accounting for the negative antiferromagnetic interactions is identical with that for the positive ferromagnetic ones since the possibility exists to have a negative exchange integral J in the Heisenberg equation (3). This may account for the magnetic interactions in metals, for instance, where the distances between paramagnetic elements are short enough to allow an overlapping of the electronic orbitals. However, a great number of antiferro- and ferrimagnetic materials are oxides, halides, or chalcogenides, in which the paramagnetic ions are separated by the anions. The extent of direct exchange is, thus, very low and does not account for the high transition temperature often observed.

B. The Superexchange Theory

The discrepancy between the theory and the experimental results has led Kramers, Van Vleck, and Anderson to consider indirect magnetic couplings between paramagnetic cations via the nonmagnetic

ions. This is termed *superexchange coupling* (*3–5, 97, 182*). Figure 1 shows typical orbitals participating in 180° superexchange interactions between two metal ions M_1 and M_2 via a ligand X by $p\sigma$ or $p\pi$ couplings.

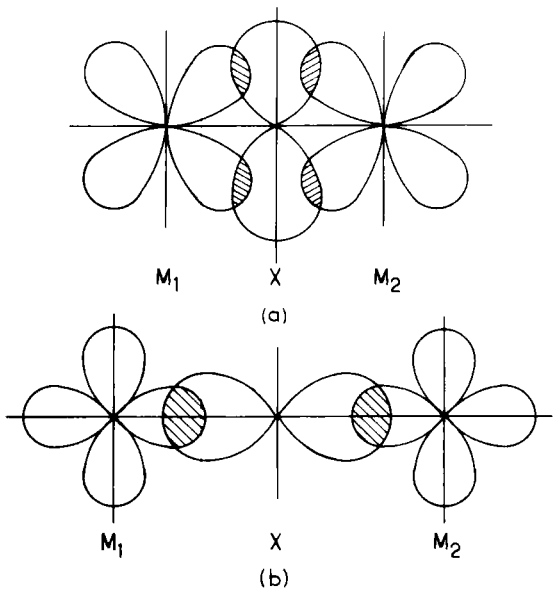

FIG. 1. Orbitals involved in 180° superexchange interactions: (a) t_{2g}—$p\pi$—t_{2g} coupling; (b) e_g—$p\sigma$—e_g coupling.

Most of the superexchange mechanisms involve spin transfers through an excited state in which an electron has hopped from one ion to another. For example, in linear Mn^{2+}—O^{2-}—Mn^{2+} bonding, several mechanisms with excited configuration admixed can be proposed:

$$Mn^{2+}—O^{2-}—Mn^{2+} + \alpha_1(Mn^{+}—O^{-}—Mn^{2+}) \quad \text{(correlation)}$$

$$Mn^{2+}—O^{2-}—Mn^{2+} + \alpha_2(Mn^{+}—O—Mn^{+}) \quad \text{(correlation)}$$

$$Mn^{2+}—O^{2-}—Mn^{2+} + \alpha_3(Mn^{+}—O^{2-}—Mn^{3+}) \quad \text{(delocalization)}$$

where α_1, α_2, and α_3 are admixture coefficients. In spite of disagreement among different authors, Anderson concluded that the third mechanism proposed by Kondo is the source of the antiferromagnetic contribution to the exchange. By using a second-order perturbation theory,

he showed that the antiparallel configuration is stabilized relative to the spin parallel one by an energy of

$$\Delta E = \frac{4b^2}{U} \tag{5}$$

where U is the energy required to form the excited $Mn^{+}—O^{2-}—Mn^{3+}$, an electron having been transferred from one manganese to the other. According to Pauli's principle, the spin of the transferred electron must be antiparallel to the electron already situated on the Mn orbital. This implies that the 1-electron Hamiltonian h can mix the excited state only into the spin antiparallel ground state. The matrix element of h has the form $b = \langle\psi_1|h|\psi_2\rangle$ and, from the perturbation theory,

$$b \simeq f_\sigma(E_d - E_p) \tag{6}$$

where f_σ is the spin transfer coefficient and $\Delta = (E_d - E_p)$ is the energy difference between the d and p orbitals [for more details, see Anderson (*3*) and Owen and Thornley (*125*)].

By analogy with the Heisenberg Hamiltonian,

$$JS_1S_2 = \frac{4b^2}{U} S_1S_2 \tag{7}$$

Briefly, one of the essential points given by almost all of the superexchange theories is that the exchange integral of $p\sigma$ bonding is [from Eqs. (6) and (7)]

$$J = f_\sigma{}^2 \left\{\frac{4(E_d - E_p)^2}{U}\right\} \tag{8}$$

This result may be extended to $p\pi$ and s bonding and described by the following two rules: (*i*) if two magnetic ions transfer unpaired spin to the same ligand orbital, then, according to Pauli's principle, the spins will be coupled antiparallel (antiferromagnetic exchange contribution); and (*ii*) if two magnetic ions transfer unpaired spin to different orbitals of the same ligand, according to Hund's rule, the spins will be coupled parallel (ferromagnetic exchange contribution). Both rules assume that the magnitude of the interaction is proportional to the probability of finding the spins simultaneously in the ligands considered (i.e., proportional to the involved spin transfer coefficients). Another consequence of this theory is that superexchange interactions

will be influenced by the M—X—M angle and will reach a maximum for an angle of 180°.

C. The Nature of Magnetic Interactions

Although theoretical results of the superexchange theory are in rather rough quantitative agreement with experiments, one of the most useful developments has been the formulation of the semiempirical theories proposed by Goodenough (*63*, *64*) and Kanamori (*87*). These allow prediction—at least in simple cases—of the nature and the sign of the magnetic interactions between different ions and for different structures.

1. Direct Cation–Cation Interactions

In most of the structures considered the transition elements are surrounded by anions that do not favor direct coupling, but direct cation–cation interactions may occur if the transition elements have extended orbitals or are in structures where the anionic polyhedra share faces or edges (Fig. 2). Three cases are considered depending on the respective filling of the overlapping orbitals.

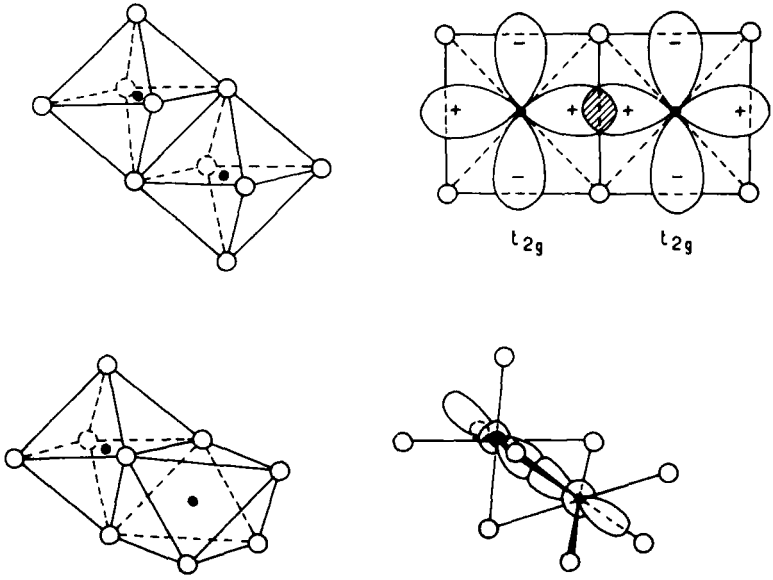

FIG. 2. Direct interactions in edge-sharing and face-sharing octahedra.

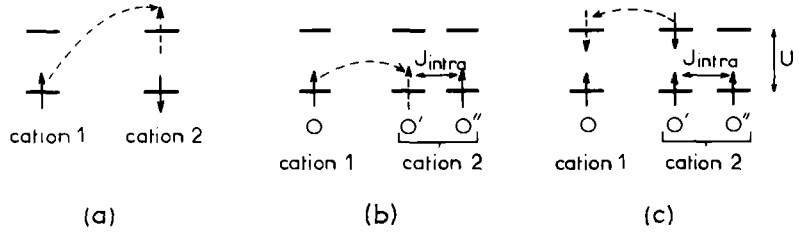

FIG. 3. Diagrams of direct interaction mechanisms.

a. Overlap of Two Half-Filled Orbitals. The corresponding exchange integral is $J = -2b^2/U$, where b is the transfer integral proportional to the orbitals overlapping, and U the energy difference between the ground and the excited states corresponding to 1 electron transfer from one cation to the other. This transfer is done without changing the sign of the spin and gives antiferromagnetic coupling (Fig. 3a).

b. Overlap of One Half-Filled Orbital O and One Empty Orbital O'. The electron transfer is spin-independent unless there is a half-filled orbital O'' orthogonal to O' on the receiving cation. The transfer integral is greater if the spin of the transferred electron is parallel to the spin of the orthogonal orbital O'' because the exchange coupling within the receiving cation is proportional to the intra-atomic exchange integral J_{intra}. The interaction is ferromagnetic and the corresponding exchange integral, which is positive, is $J = +2b^2J_{intra}/U^2$ (Fig. 3b).

c. Overlap of One Half-Filled Orbital O and a Full Orbital O'. The only electron transfer possible is from O' to O, and the spin of the transferred electron must be antiparallel to the spin of O. The presence of a partially filled orbital O'' orthogonal to O' favors transfer to O of the electron of O' antiparallel at O''. The atomic moments are coupled ferromagnetically; the exchange integral is $J = 2b^2J_{intra}/U^2$ (Fig. 3c).

2. Indirect Cation–Anion–Cation Interactions

a. Symmetry Rules of Superexchange. We saw previously the different types of superexchange couplings:

i. Delocalization superexchange, which is characterized by the transfer of 1 electron from a cation to a cation via the anion. It has the same sign as the corresponding direct coupling.

ii. Correlation superexchange, which results from a simultaneous transfer of 2 electrons of one anionic orbital to two cationic orbitals.

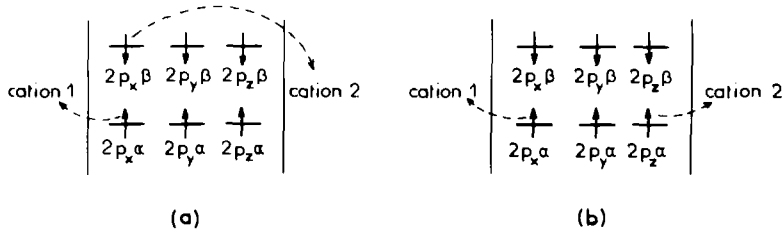

FIG. 4. Simple (a) and double-correlation (b) couplings.

However, the transferred electrons can arise from two different anionic orbitals (double-correlation superexchange) (Fig. 4). In the first case the spins of the transferred electrons are antiparallel; in the second, they are parallel because of Hund's rule. Whatever the coupling mechanism may be, the transfer integral characterizing the overlapping of the cationic and anionic orbitals must not be nil. A noticeable interaction will occur if the orbitals are not orthogonal. For cations of transition elements in sixfold coordination, there are only electron transfers between anionic $p\sigma$ and cationic e_g orbitals (σ transfer) and anionic $p\pi$ and cationic t_{2g} orbitals (π transfer). The σ transfer is more important than π transfer owing to a greater orbital overlap (Fig. 1).

b. 180° Interactions. Such interactions occur for corner-sharing octahedra. Figure 5 summarizes the different 180° interactions that could

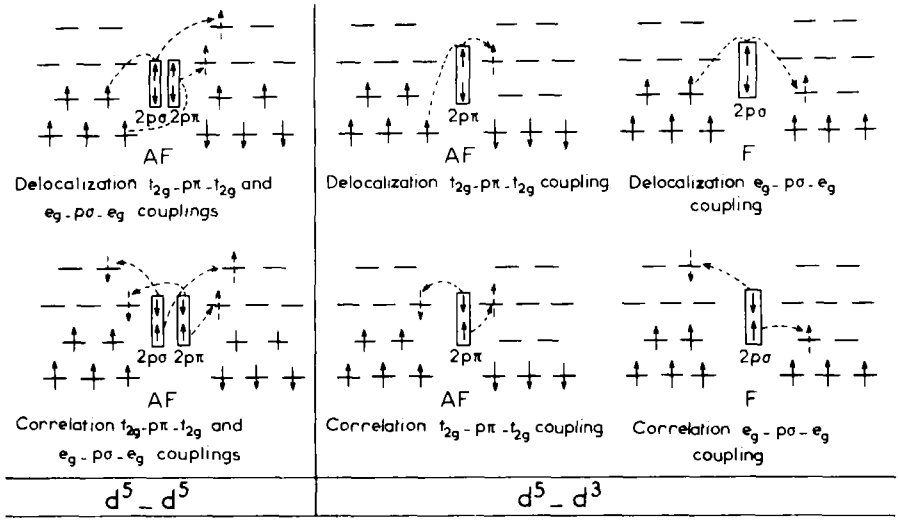

FIG. 5. Various 180° interaction mechanisms.

appear in two significant cases: d^5–d^5 (half-filled t_{2g} and e_g orbitals) and d^3–d^5 (half-filled t_{2g} and empty e_g orbitals for one cation, and half-filled t_{2g} and e_g orbitals for the other).

c. 90° Interactions. These interactions occur when octahedra share edges or faces. For this reason the 90° interaction coexists with the direct interaction (Fig. 6). The 90° interaction may occur either by double correlation between two t_{2g} orbitals (t_{2g}–$p\pi$–$p\pi'$–t_{2g}) or two e_g orbitals (e_g–$p\sigma$–$p\sigma'$–e_g), or between one t_{2g} orbital and one e_g orbital (t_{2g}–p–e_g) via only one anionic orbital. The first case is never taken into account because it is dominated by the direct t_{2g}–t_{2g} coupling. The 90° double-correlation couplings between two identical ions are ferromagnetic owing to Hund's rule.

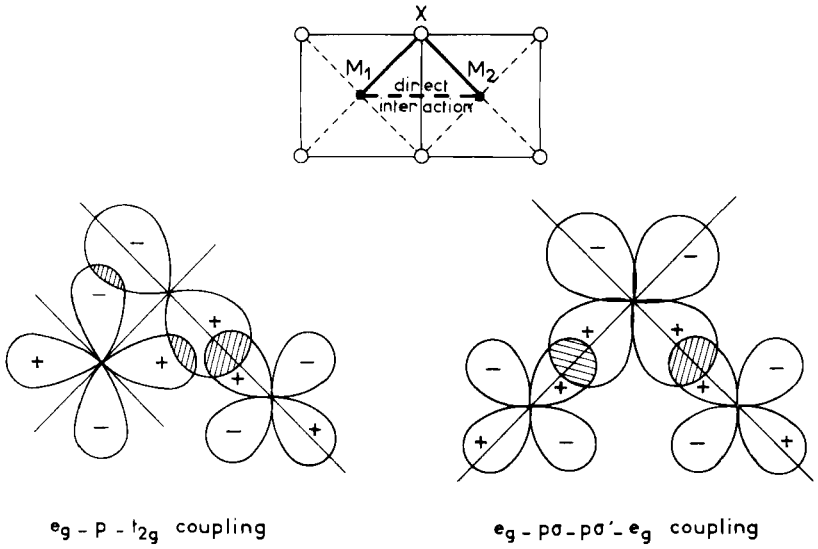

FIG. 6. The 90° superexchange interactions.

d. Intermediate Angles. Magnetic interactions with cation–anion–cation angles intermediate between 90° and 180° are often present (spinel, rutile structures, etc.). The previous considerations are no longer valid, and the participating orbitals are more difficult to determine (*64*). One may consider that for angles between 150° and 180°, the 180° interactions rules are convenient; similarly, for angles between 70° and 120°, the 90° interactions rules may be applied (*173*).

III. Ferrimagnetic Fluorides

A. From Ferrimagnetism in Oxides to Ferrimagnetism in Fluorides

Néel showed that the presence of a spontaneous magnetization was not necessarily due to ferromagnetic behavior. By generalizing the molecular field concept, he could explain the magnetic properties of the ferrites using the hypothesis of parallel and antiparallel interactions between two different crystallographic sites constituting real sublattices (*119*).

1. Ferrimagnetism in Oxides

Since their discovery by Néel, the properties of the ferrimagnetic oxides have been widely studied. Ferrimagnetism arises mainly owing to the possibility of a transition element to be situated in different coordination polyhedra (octahedral, tetrahedral, dodecahedral, etc.).

Among the various types of ferrimagnetic ferrites, we find the following:

i. The spinels with the general formula AB_2O_4. Their structure involves tetrahedral [A] and the octahedral [B] sites that contain the transition elements and which are unequal in number (Fig. 7).

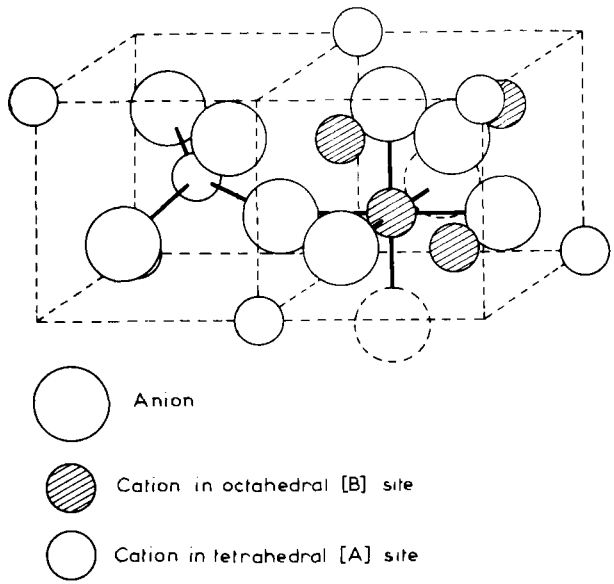

FIG. 7. Interactions in the spinel structure.

Ferrimagnetism occurs when there are interactions between the [A] and [B] sites (*68*, *120*, *157*).

ii. The garnets $Ln_3M_5O_{12}$ (Ln = rare earth, M = transition element) whose structure has been determined by Bertaut and Forrat (*16*). Their magnetic properties have been explained by Pauthenet (*1*, *17*, *126*, *127*). Their structure has three nonequivalent sites: octahedral (*a*), tetrahedral (*d*), and dodecahedral (*c*); the last contains the rare earth (Fig. 8). The number of the different sites corresponds to the ratio 2:3:3. Ferrimagnetism is assured only by the presence of paramagnetic cations in both octahedral and tetrahedral sites.

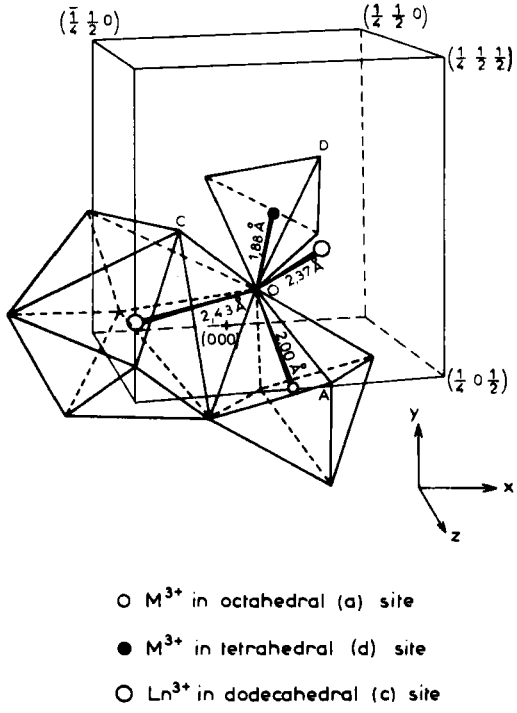

FIG. 8. Cationic and anionic surroundings in the $Y_3Fe_5O_{12}$ garnet structure.

iii. The hexagonal ferrites with the magnetoplumbite structure $AFe_{12}O_{19}$ (A = Ba, Sr). They have three different types of site for the iron atoms, namely octahedral, tetrahedral, and trigonal bipyramidal. The 12 iron atoms are distributed in an unequal number leading to ferrimagnetism. A partial substitution of the A cation by a transition ele-

ment (Ni^{2+}) also gives ferrimagnetic compounds. These ferrites are characterized by strong remanent magnetization and a high coercivity due to the large anisotropy (*120*, *156*, *191*).

2. Substitution of Oxygen by Fluorine

The substitution of oxygen by fluorine in the spinel and garnet structures has been widely studied, particularly by Portier and his collaborators. These studies have given more information about the precise nature of the magnetic couplings and conduction mechanisms which were not clearly explained for the totally oxygenated compounds. Generally, the proportion of fluorine introduced is low, and the structure of the compound obtained is identical with that of the oxide used as starting material.

The study of the oxyfluorinated spinels showed various substitution mechanisms. In oxyfluorospinels with the formula

$$M_a^{3+}Fe_b^{3+}\ \square_c\ O_{4-x}F_x$$

[M^{3+} = 3*d* element, $a + b + c = 3$, and $2a + 3b = 2(4 - x) + x$], replacement of oxygen by fluorine is compensated by the substitution of Fe^{3+} by Fe^{2+}, on the one hand, and by the presence of cationic vacancies, on the other (*58*). In $Cu^{2+}_{1+x}Fe^{3+}_{2-x}O_{4-x}F_x$ ($0 \leq x \leq 1$), oxygen–fluorine substitution is compensated by replacement of Fe^{3+} by Cu^{2+} (*137*). Stoichiometric oxyfluorospinels $M^{2+}Fe^{2+}Fe^{3+}O_3F$ (M^{2+} = 3*d* transition element) have also been reported (*28*). Recently, a general study of the magnetic interaction mechanisms and electrical properties of oxyfluorospinels has been made by Claverie *et al.* (*32*, *33*).

In the garnet structure, the substitution possibilities are more numerous. The charge compensation required by O—F substitution is achieved by replacing the rare earth ions in the *c* sites by divalent cations in the $Ca_xY_{3-x}Fe_5O_{12-x}F_x$ (*83*) and $Ca_xLn_{3-x}Fe_5O_{12-x}$ (*56*) series. Charge compensation can also be made in the *a* and *d* sites, e.g., in the $Ln_3Fe^{3+}_{3-x}M_x^{2+}O_{12-x}F_x$ series prepared by Portier *et al.* (*135*, *170*) (Ln = Y, Gd; M = 3*d* element), or simultaneously in the three sites, for instance in the $Y_{3-3x}Ca_{3x}Fe^{3+}_{5-x}M_x^{4+}O_{12-x}F_x$ (M = Si, Ti, Sn) and $Y_{3-3x}Ca_{3x}Fe^{3+}_{5-x}M_x^{5+}O_{12-x}F_x$ (M = V, Nb) series studied by Tanguy *et al.* (*114*, *115*). These oxyfluorinated garnets present some advantages compared to the oxygenated ones, namely lower synthesis temperature and a decrease in the cost of the doubly substituted garnets owing to the replacement of yttrium by calcium.

From a magnetic point of view when the starting oxygenated ferrite is ferrimagnetic, the oxyfluorinated series is also ferrimagnetic and

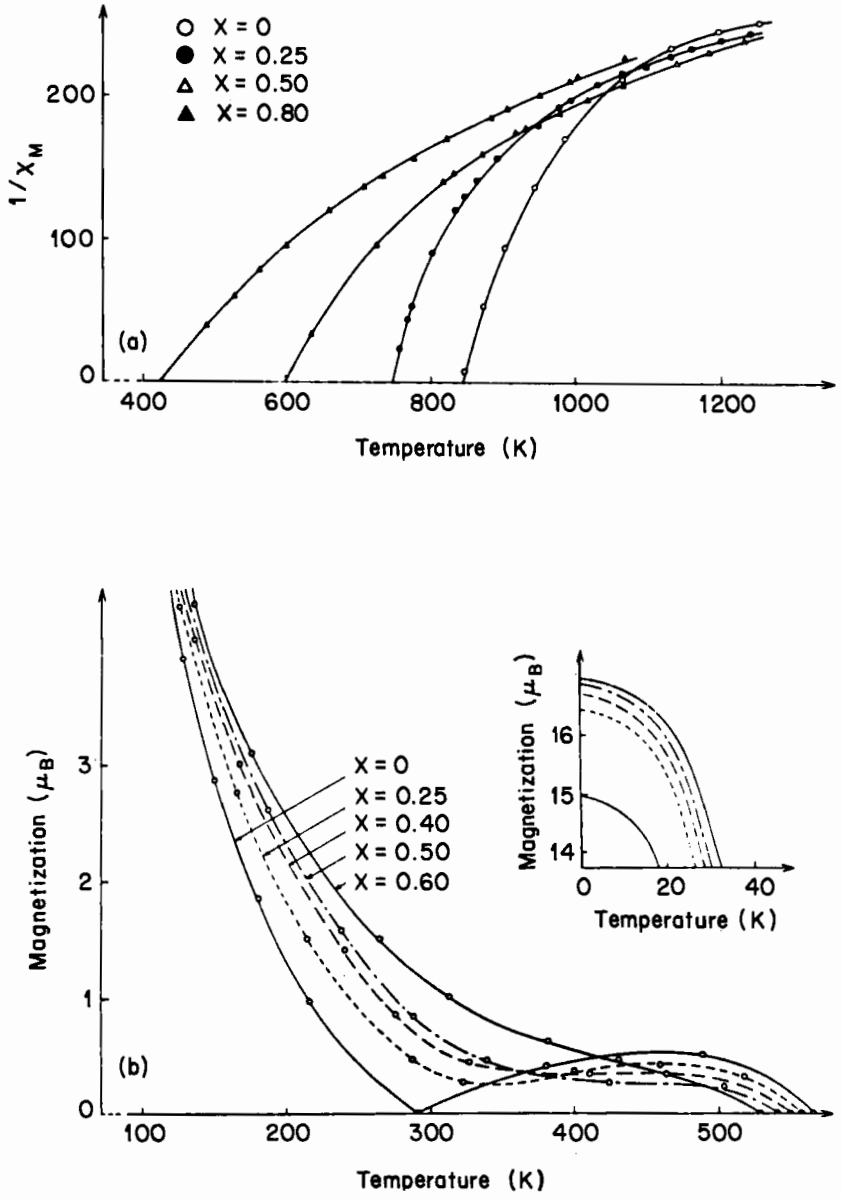

FIG. 9. (a) Temperature dependence of the reciprocal molar susceptibility of oxyfluorospinels $Zn_xFe_{1-x}[NiFe]O_{4-x}F_x$ (*32*); (b) the spontaneous magnetization of oxyfluorogarnets $Gd_3Fe_5O_{12-x}F_x$. [From Portier *et al.* (*135*), by permission of Gauthiers-Villars.]

a decrease of the Curie temperature is observed in all cases (Fig. 9). A large substitution has never been obtained. This decrease is essentially due to the replacement of one transition element by another with a smaller spin. Fluorine, which is more electronegative and less polarizable than oxygen, gives weaker superexchange couplings but does not really influence the magnetic order temperature.

3. Conditions for Obtaining Ferrimagnetism in Fluorides

Owing to the amazing development of the ferrites, it was tempting to apply the conditions leading to ferrimagnetism in oxides to the corresponding fluorides. This was not easy because in the oxides the transition elements can possess a coordination number of 4, 6, or 8, whereas they usually have sixfold coordination in the fluorides.

Some entirely fluorinated garnets and spinels are known. In the spinels Li_2NiF_4(*140*) and Li_2CuF_4 (*71*), the lithium atoms occupy all the tetrahedral and half of the octahedral sites, the other half being occupied by nickel or copper. Ferrimagnetism cannot occur because there is no longer magnetic interactions between the [A] and the [B] sites and the two compounds are paramagnetic.

Likewise, some fluorinated garnets $Na_3Li_3M_2^{2+}F_{12}$ (M = transition element) have been prepared by de Pape *et al.* (*44*). The transition element is situated exclusively in the octahedral sites (*a*) with lithium in the tetrahedral sites (*d*) and sodium in the dodecahedral sites (*c*). Ferrimagnetism cannot be present because the transition elements occupy only one type of site and the interactions between two *a*-type sites are very weak. These garnets are also paramagnetic.

Ferrimagnetism is only liable to occur in fluorides if, in addition to the presence of at least two different crystallographic sites for the transition element, an order exists between the fluorinated octahedra. But this condition is not sufficient since exact compensation of the sublattices would lead to antiferromagnetism. The following two general rules can be deduced.

1. If the number of different sites is equal, the presence of two transition elements with different electronic structures (e.g., weberite Na_2NiFeF_7) or with a difference in the occupation of these sites (e.g., $MnAl_{1-x}Fe_xF_5$) is necessary:

$$\underset{\text{(site 1)}}{x\mathbf{M}} - \underset{\text{(site 2)}}{x\mathbf{M}'} \xrightarrow{\mathbf{M} \neq \mathbf{M}'} \text{ferrimagnetism}$$

or

$$x\mathbf{M} - (x - \varepsilon)\mathbf{M}' \longrightarrow \text{ferrimagnetism}$$

2. When the number of sites is unequal, ferrimagnetism is observed even if they are occupied by identical paramagnetic ions (e.g., chiolite $Na_5Fe_3F_{14}$, $6H$ $CsMF_3$):

$$x\mathbf{M} - y\mathbf{M} \xrightarrow{x \neq y} \text{ferrimagnetism}$$

4. The Ferrimagnetic Fluorides Series

Although the ferrimagnetic oxides have been known for more than 3000 years, it was only in 1958 that Knox and Geller discovered the first ferrimagnetic fluoride, $Na_5Fe_3F_{14}$, with the chiolite type of structure (*92*). About 10 years later Shafer *et al.* (*146*) and, independently, Smolensky *et al.* (*158*) discovered the ferrimagnetism of $RbNiF_3$ with the hexagonal $BaTiO_3$ type of structure. During the 1967–68 period, new AMF_3 ferrimagnetic fluorides were found in Leningrad, Tokyo, and Bordeaux. A third type of ferrimagnetic fluoride, the weberite-type $Na_2M(II)M(III)F_7$ [M(II), M(III) = 3*d* transition elements], was discovered simultaneously by Cosier and Wise and by Tressaud, Grannec, Olazcuaga, and Portier (*35*).

More recently, two new series of fluorides were found to be ferrimagnetic: $M(II)M(III)F_5$ compounds with the $MnAlF_5$ or Cr_2F_5 structure by Tressaud *et al.* (*175*), and $Cs_2M(II)M'(II)F_6$ compounds [M(II), M′(II) = 3*d* transition elements] with the Ba_2NiTeO_6 (12*R*) type, derived from the hexagonal perovskites by Dance *et al.* (*41*).

B. Experimental Methods

1. Preparative Methods

The high reactivity of fluorine explains the specific nature of the experimental methods used. The main difficulties are due to the physicochemical properties of fluorine and of its derivatives, namely strong corrosive effects on almost all materials, an ease of hydrolysis, and a high volatility.

Several reviews of the preparative methods of the solid fluoro compounds have appeared (*15, 19, 91, 128, 153*). The most important methods used to prepare ferrimagnetic fluorides will be summarized in the following sections.

a. Reactions in Solution. The solvents used may be either aqueous HF at ambient or high pressure (hydrofluorothermal synthesis) or nonaqueous solvents such as BrF_3, BrF_5, and SbF_5. For instance, $TlNiF_3$ was first synthesized by dissolving equimolecular mixtures of

TlOH and $Ni(OH)_2$ in hydrofluoric acid and firing the product at 350°C in a stream of nitrogen gas (*95*).

b. Gas–Solid Reactions. The fluorides of the transition metals are frequently hygroscopic and generally have a marked tendency to form hydrates or hydroxyfluorides. Because of the difficulties of obtaining anhydrous products with the former method, it is necessary in most cases to work under strictly anhydrous conditions. Several types of "fluorination lines" using F_2, HF, or other fluorinating agents have been described (*15, 19, 69, 70, 128*). Fluorination by fluorine and by gaseous hydrogen fluorine constitutes one of the main methods for synthesizing solid fluorinated compounds (Table I). The preparation of monovalent silver compounds requires several fluorinations at 80°C (to avoid the formation of divalent silver) followed by refirings at low temperature (200°C) in sealed gold tubes.

TABLE I

EXAMPLES OF FLUORINATION REACTIONS[a]

$5NaF + 3M(II)Cl_2 \xrightarrow{F_2,\ 500°C}$	$Na_5M_3(III)F_{14}$ (M = 3*d* transition element)
$5NaF + 2FeF_3 + CoF_2 \xrightarrow{F_2,\ 500°C}$	$Na_5Fe_2CoF_{14}$
$CsF + M(II)Cl_2 \xrightarrow{HF,\ 600°C}$	$CsM(II)F_3$ (M = Fe, Co, Ni)
$2NaF + M(II)F_2 + CoF_2 \xrightarrow{F_2,\ 500°C}$	$Na_2M(II)CoF_7$ (M = Mg, Ni)
$AgNiF_3 + Ag + M(III)F_3 \xrightarrow[\text{and refirings}]{F_2,\ 80°C}$	$Ag_2NiM(III)F_7$ (M = Al, Cr, Fe)
$3LiF + 3NaF + 2CoO \xrightarrow{F_2,\ 500°C}$	$Li_3Na_3Co_2F_{12}$ (Ref. *44*)

[a] From Dance (*39*).

c. Solid–Solid Reactions. i. *At low pressures.* Ternary fluorides of transition metals are also often prepared from the binary fluorides in a direct solid-phase synthesis. Although this method does not differ hardly from conventional chemical synthesis, some precautions should be taken: in most cases the mixture must be ground in a dry atmosphere because of its hygroscopic nature and heated in an argon-sealed nickel, platinum, or gold tube.

ii. *At high pressures.* High-pressure techniques have been of the greatest use in the field of ferrimagnetic fluorides. We will see later the effect of the pressure on the crystallographic and magnetic properties of AMF_3 compounds (*104*). Pressure may be applied by using belt

TABLE II

CRYSTAL GROWTH OF FERRIMAGNETIC FLUORIDES

Compound	Crystal growth technique	Maximal temperature and experimental conditions	Shape and dimensions (mm)	Color	Ref.
$CsMnF_3$	Modified Bridgman-Stockbarger	900°C, in HF atmosphere	3 × 3 × 1	Pink	(*204*)
$CsFeF_3$	Bridgman-Stockbarger	800°C	0.5 × 0.5 × 0.5	Colorless	(*90, 109*)
$RbNiF_3$	Bridgman-Stockbarger	1055°C	—	Yellow–green	(*146*)
	Bridgman-Stockbarger	960°C	15 × 5 × 5	Yellow–green	(*158*)
	Bridgman-Stockbarger	—	Elliptical, 10 cm^3	Yellow–green	(*2, 73*)
$RbNi_{1-x}Co_xF_3$	Bridgman-Stockbarger Chloride flux	900°C, $3RbHF_2 + (1-x)NiCl_2 + xCoCl_2 \rightarrow RbNi_{1-x}Co_xF_3 + 2RbCl + 3HF$	—	From yellow–green to light pink	(*52*)
$Na_5Cr_3F_{14}$	Chloride flux	750°C, $5NaCl + 5CoCl_2 + 3CrF_3 + 5NaF \rightarrow Na_5Cr_3F_{14} + 5NaCl + 5CoCl_2$	Prismatic, 2 × 2 × 2	Dark green	(*113*)
$Na_5Fe_3F_{14}$	Chloride flux	600°C, in 40% NaCl–60% $CoCl_2$ (in mole) flux	Prismatic, 2 × 2 × 1	Brown	(*178*)
$Na_2Ni(II)Cr(III)F_7$	Chloride flux	600°C, $7NaCl + M(II)Cl_2 + 4M(II)F_2 + 2FeF_3 \rightarrow 2Na_2M(II)FeF_7 + 3NaCl + 3M(II)Cl_2$ [with M(II) = Cr, Mn, Ni]	Prismatic, ~1 mm^3	Dark green	(*112*)
$Na_2Mn(II)Fe(III)F_7$	Chloride flux		Parallelepipedic, 2 × 3 × 2	Light brown	(*178*)
Na_2NiFeF_7	Chloride flux		Prismatic, 2 × 2 × 1	Light green	(*112, 178*)

apparatus, tetrahedral anvil press, etc. (*22*, *75*). It is important for the reactants to be placed in gold or platinum containers to avoid corrosion of the apparatus.

iii. *Crystal growth*. The techniques used to grow single crystals of ferrimagnetic fluorides are essentially the Bridgman–Stockbarger method and the flux method (Table II; Fig. 10). The latter can be carried out in an inert or a reducing atmosphere (*60*, *61*) and allows lower reaction temperatures (*121*, *178*).

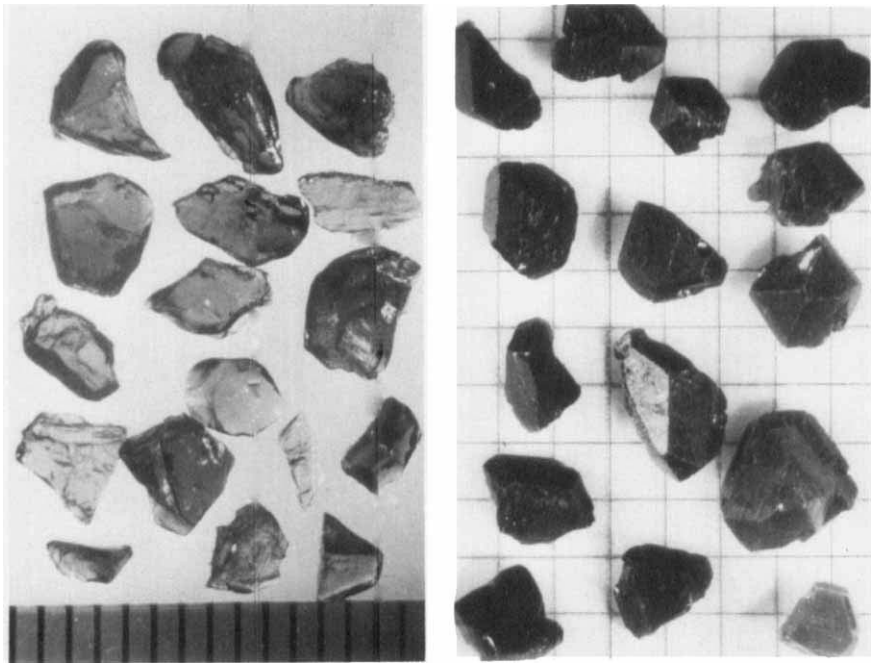

FIG. 10. Crystals of Na_2MnFeF_7 (left) and $Na_5Fe_3F_{14}$ (right) obtained by flux techniques. [From Dance (*39*).]

2. *Physical Techniques*

A large number of different techniques lead to information on specific physical parameters and improve the understanding of the properties of magnetic compounds. They can be divided into four general groups: magnetization measurements, resonance phenomena, neutron diffraction, and optical and magneto-optical spectroscopy. Table III summarizes the different types of techniques and gives the parameters that

TABLE III

SUMMARY OF PHYSICAL TECHNIQUES EMPLOYED WITH MAGNETIC COMPOUNDS

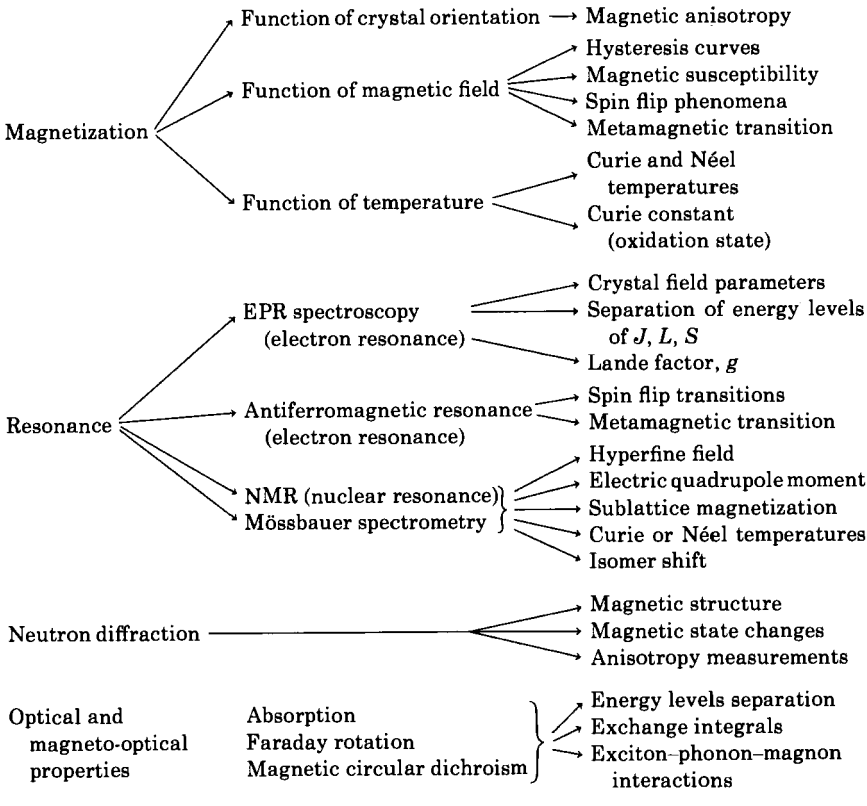

can be deduced from the experimental data. A more complete survey of the techniques of magnetochemistry has been given by Schieber (*144*).

C. Compounds with General Formulas AMF_3 and $A_2MM'F_6$

The major part of the investigations of different series of ferrimagnetic fluorinated compounds were concerned with the study of the physical properties of phases with "hexagonal perovskite" type. The structures of AMF_3 hexagonal phases can be deduced from the various arrangements of the cationic and anionic layers (A), (B), or (C) (Fig. 11a). The articles of Wells (*190*) and Katz and Ward (*89*) have

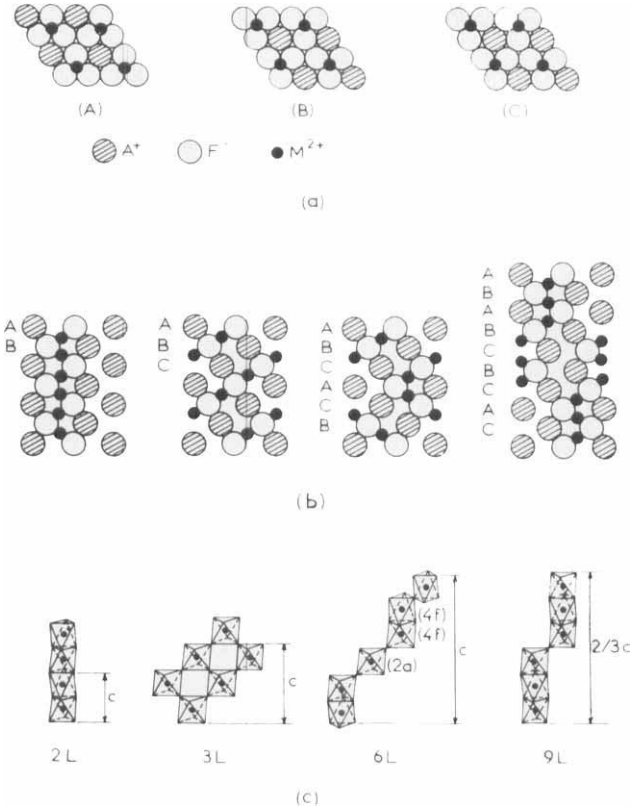

FIG. 11. Cationic and anionic arrangements in cubic and hexagonal perovskite fluorides.

shown that the number of combinations is quite endless. Although there are a great number of different hexagonal structures for the AMO_3 oxides, only a limited number of structural types have so far been identified for AMF_3 fluorides.

Among the authors who studied this particular problem, Babel has presented a classification of the hexagonal structures derived from that of perovskite (*8*, *9*). Generally these phases are characterized by the number of layers that constitute the stacking sequence. Figure 11b and c shows in addition to the cubic perovskite structure, which is named $3L$ (or $3C$ because of the cubic symmetry), the two-layer $2L$ (or $2H$, H for hexagonal), six-layer $6L$ ($6H$), nine-layer $9L$ (or $9R$, R for rhombohedral symmetry) lattices. All the hexagonal fluorides derived from the perovskite structure are collected in Table IV.

TABLE IV

HEXAGONAL A(I)M(II)F_3 PHASES[a]

Structure type	$BaNiO_3$ (2*L*)	$BaRuO_3$ (*9L*)	$BaTiO_3$ (6*L*)	Ba_2NiTeO_6 (12*L*)
Crystallographic data	a = 5.580 Å c = 4.832 Å (*C6mc*) (*100*)	a = 5.75 Å c = 21.60 Å ($R\bar{3}m$) (*47*)	a = 5.735 Å c = 14.05 Å ($P6_3/mmc$) (*25*)	a = 5.797 Å c = 28.595 Å ($R\bar{3}m$) (*94*)
Hexagonal AMF_3 phases	$CsNiF_3$ (*7, 8*) $CsCuF_3$ (*7*) (Related structure)	$CsCoF_3$ (*9, 141*) $(Rb_{0.25}Cs_{0.75})NiF_3$ (*42*)	$CsMnF_3$ (*154, 204*) $CsFeF_3$ (*90*) $(Rb_{0.5}Cs_{0.5})CoF_3$ (*42*) $RbNiF_3$ (*142*) $TlNiF_3$ (*95*) $RbZnF_3$ (*145*) $TlZnF_3$ (*145*)	$Rb_2LiM(III)F_6$ (*11, 72*) $Cs_2NaM(III)F_6$ (*11, 72*) $Cs_2MnM(II)F_6$ (*41*) $Cs_2CdM(II)F_6$ (*41*)

[a] Italic numbers in parentheses are reference citations.

According to the rules given in Section III,A, the only known types of fluorides liable to present ferrimagnetic properties are the $6H$ and $12R$ phases, in which at least two different and nonequivalent crystallographic sites for the $3d$ elements are present.

1. *$BaTiO_3$-Type (6H) Phases*

In 1962, Rüdorff, Kandler, and Babel prepared $RbNiF_3$ and showed that it had the hexagonal structure of $BaTiO_3$ (*141*). A great number of crystallographic studies of single crystals have been undertaken since then on $RbNiF_3$ or similar compounds (Table IV) (*6*, *10*, *188*). A low-temperature crystallographic study shows no structural modification down to 30 K (*165*).

The ferrimagnetism of the hexagonal $BaTiO_3$-type fluorides was first discovered for $RbNiF_3$ (*146*, *158*). During the years 1967–68 this property was also observed for $TlNiF_3$ by Kohn *et al.* (*95*), for $CsFeF_3$ by Portier *et al.* (*133*) and by Eibschütz *et al.* (*51*), and for NH_4NiF_3 by Shafer and McGuire (*147*). Ferrimagnetism is due to the presence of two nonequivalent $2a$ and $4f$ sites for the divalent cation. If we consider the exchange between the nearest neighbors, two types of interactions exist in the lattice: the first, between the transition elements situated in the $2a$ and $4f$ sites and, the second, between those situated in two $4f$ sites. According to Anderson's theory the former is due to 180° superexchange couplings, and the latter introduces both direct and 90° superexchange couplings. For the elements studied (d^4 to d^8), the 180° couplings are essentially antiferromagnetic, whereas the interaction within the (M_2F_9) groups are mostly influenced by ferromagnetic couplings except in the case of $CsMnF_3$, where the d^5–d^5 90° couplings are strongly antiferromagnetic. Consequently, $CsMnF_3$ is antiferromagnetic (*102*, *202*).

The signs of the magnetic couplings have been checked by neutron diffraction, by Pickart and Alperin for instance for $RbNiF_3$, $CsFeF_3$ (*130*), and $CsMnF_3$ (*129*). The angle between the moment's direction and the c axis is 90° for $RbNiF_3$ and $CsMnF_3$, and 75° for $CsFeF_3$. The nature of the couplings and the direction of the spins are given in Table V. A neutron inelastic scattering study has given the value of the two exchange integrals (*2*):

$$|J_{2a-4f}| = 64.8\ \text{cm}^{-1} \qquad \text{and} \qquad |J_{4f-4f}| = 14.7\ \text{cm}^{-1}$$

The Mössbauer spectrum of $CsFeF_3$ measured by Eibschütz *et al.* (*51*) shows that above T_c the intensity of the two different absorption

TABLE V

MAGNETIC STRUCTURES OF 6L AMF_3 FLUORIDES

Compound	Signs of magnetic coupling		Direction of spin axis	Technique	Ref.
	$(2a)-(4f)$	$(4f)-(4f)$			
$CsMnF_3$	−	−	$\perp c$	Neutron diffraction	(*129*)
$CsFeF_3$	−	+	75° from c	Anisotropy Neutron diffraction	(*108*, *130*)
$RbNiF_3$	−	+	$\perp c$	Magnetization measurements Neutron diffraction	(*130*, *146*)
$RbNi_{1-x}Co_xF_3$ $0 \leqslant x \leqslant 0.25$	−	+	$\perp c$ → $\parallel c$ (for $x = 0$) (for $x = 0.25$) cone angles	Magnetization and magneto-optic measurements	(*52*, *167*)
$RbMg_{1-x}Co_xF_3$ $0.35 \leqslant x \leqslant 0.68$	−	+	$\parallel c$	Anisotropy measurements	(*148*)
$RbCo_{0.2}Ni_{0.8-y}Ca_yF_3$	−	+	Cone angles	Anisotropy measurements	(*108*)

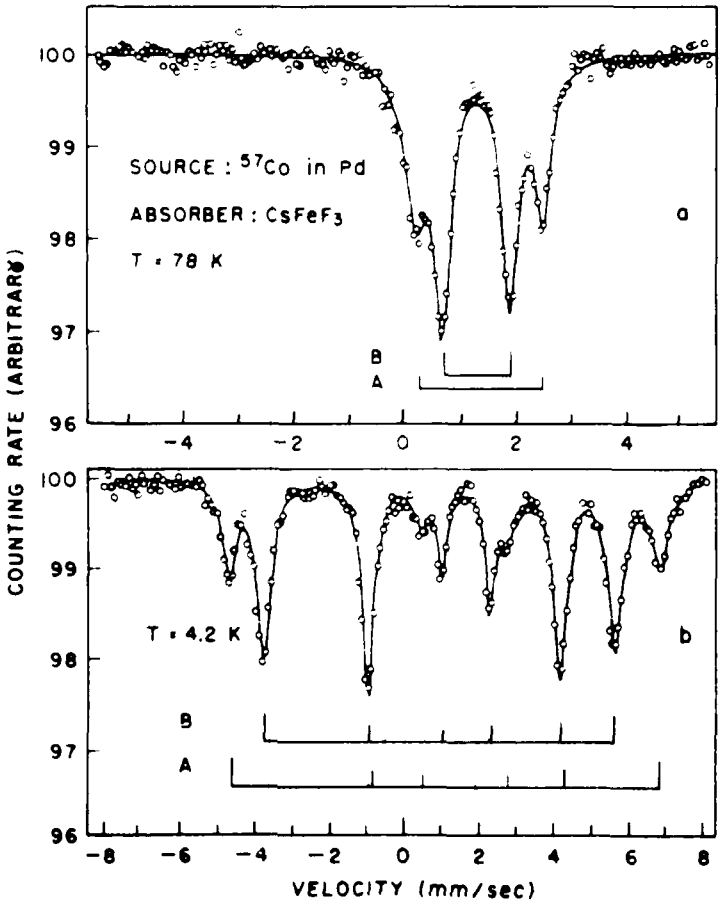

FIG. 12. Mössbauer spectra of $CsFeF_3$. [From Eibschütz *et al.* (*51*), by permission of the American Institute of Physics.]

lines is in the ratio 2:1 (Fig. 12). In the magnetic state, the principal axis of the electric field gradient makes an angle of 40° with the direction of the hyperfine magnetic field, as was previously observed for the perovskite $RbFeF_3$ (*81*, *194*).

Shafer and McGuire found the existence of compositions of the 6*L* type having ferrimagnetic properties by studying the solid solutions $RbMg_{1-x}Co_xF_3$ (*148*) and $RbNi_{1-x}Co_xF_3$ (*107*, *167*). The Curie temperatures vary regularly with the rate of substitution. The magnetic parameters of ferrimagnetic fluorides with the 6*L* structure are shown in Table VI.

TABLE VI

MAGNETIC PARAMETERS OF 6*L* FERRIMAGNETIC FLUORIDES

6*L* Compound	T_c (K)	$\sigma_{s,0}$ (μ_B)	θ_p (K)	Ref.
$CsFeF_3$	60	1.31	−100	(*133*)
	62	1.40	−85	(*51*)
$RbNiF_3$	145	—	−130	(*158*)
	139	0.76	−300	(*18*, *146*)
$TlNiF_3$	150	0.42 (at 77 K)	—	(*95*)
NH_4NiF_3	150	0.1	—	(*147*)
$RbNi_{1-x}Co_xF_3$ $0 \leq x \leq 0.25$	139 (for $x = 0$) 115 (for $x = 0.25$)	Varies irregularly	—	(*167*)
$RbMg_{1-x}Co_xF_3$ $0.35 \leq x \leq 0.68$	10 (for $x = 0.35$) 35 (for $x = 0.68$)	Increases with x $\sigma_{s,0} = 0.48$ (for $x = 0.35$) $\sigma_{s,0} = 0.75$ (for $x = 0.68$)	—	(*148*)
$(Rb_{0.5}Cs_{0.5})CoF_3$	62	0.70	−135	(*42*)

Some studies of magnetocrystalline anisotropy on phases of the 6*L* type (*52*, *53*, *85*, *108*, *109*), whether substituted or not, have allowed the determination of the various anisotropy constants, the directions of easy magnetization, and the variations of easy magnetization cones with the substitution rate and the applied magnetic field (Table VII). As for the series $RbCo_{0.2}Ni_{0.8-y}Ca_yF_3$, in which Co^{2+} and Ca^{2+} ions have a preference for the 2*a* sites, the results showed a difference between the anisotropies of Co^{2+} in the 2*a* sites and in the 4*f* sites which are of lower symmetry, K_2 having a high positive value (Fig. 13). The crystal field parameter D_q and the spin-orbit coupling constant were determined from optical absorption measurements. In the $RbMg_{1-x}Co_xF_3$ system, where two-thirds of the CoF_6 octahedra share their faces, the values of D_q (870–880 cm^{-1}) show that the strength of the crystal field exerted on Co^{2+} is not very different from the one found in the perovskites $KCoF_3$ and $RbCoF_3$, where only corners are shared (*148*).

Compounds $CsFeF_3$ and $RbNiF_3$ are perfectly transparent ($\alpha \leq 1$ cm^{-1}) over a great part of the visible spectrum (between 20,000 and 125,000 cm^{-1} and between 20,000 and 165,000 cm^{-1}, respectively (*109*, *146*).

Faraday rotation measurements, made on $RbNiF_3$ and $CsFeF_3$, for instance, showed a magneto-optical resonance due to the $^1T_2{}^a$ transition (22,000 cm^{-1}) (Fig. 14). For $RbNiF_3$, the highest rotation (77 K, 20 kOe) is 400 deg/cm at 20,400 cm^{-1} (*132*, *146*) and for $CsFeF_3$ (80 K, 22 kOe) the rotation is 300 deg/cm at 25,000 cm^{-1} (*109*).

TABLE VII

ANISOTROPY CONSTANTS

Compound	Anisotropy constants (erg/cm^3) K_1	K_2	Cone angle	Ref.
$CsFeF_3$	-7.8×10^6	2.2×10^7	25°	(*108*)
$RbNiF_3$	-6.1×10^5 -1.4×10^6	4.46×10^4 0.3×10^6	90° ($\perp c$) 90° ($\perp c$)	(*52*) (*167*)
$RbNi_{1-x}Co_xF_3$ $0 \leq x \leq 0.35$	Increases with x $x = 0.25$, $K_1 = -2 \times 10^5$	Increases with x $x = 0.25$, $K_2 = 2.4 \times 10^6$	From 90° to 0° ($\|c$)	(*167*)
$RbMg_{1-x}Co_xF_3$ $0.35 \leq x \leq 0.68$	Increases with x $x = 0.41$, $K_1 = 2.2 \times 10^6$ $x = 0.65$, $K_1 = 8.9 \times 10^6$	Not measurable	0° ($\|c$)	(*148*)
$RbCo_{0.2}Ni_{0.8-y}Ca_yF_3$	Increases with y $y = 0$, $K_1 = -5 \times 10^5$ $y = 0.14$, $K_1 = -2 \times 10^5$	Decreases with y $y = 0$, $K_2 = 15 \times 10^5$ $y = 0.14$, $K_2 = 1 \times 10^5$	For $RbNi_{0.76}Co_{0.2}Ca_{0.04}F_3$, $\theta = 25°$	(*109*)

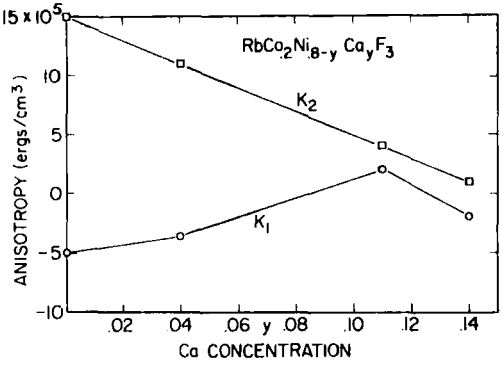

FIG. 13. Variation of anisotropy constants. [From McGuire and Shafer (*109*), by permission of the *Journal de Physique*.]

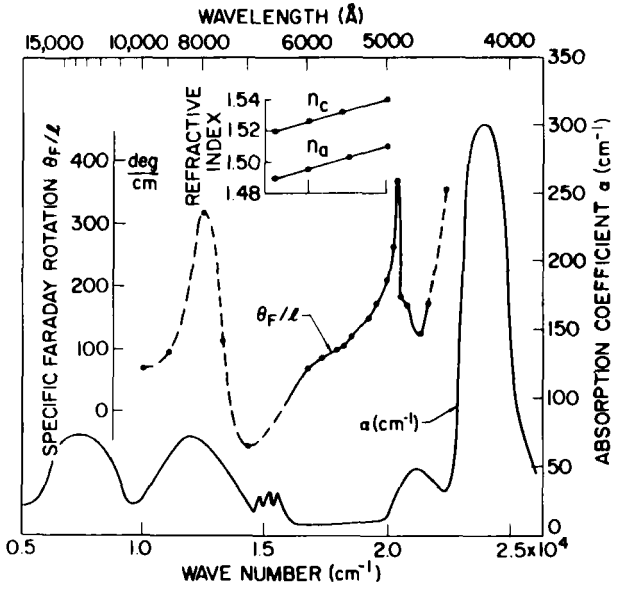

FIG. 14. Optical properties of $RbNiF_3$ single crystal. Solid lines: absorption spectrum (α) and specific Faraday rotation (θ_F/l). Insert: indices of refraction vs wavelength. [From Shafer *et al.* (*146*), by permission of the American Institute of Physics.]

In order to find the origin of exciton and magnon side bands, many polarized optical absorption and Zeeman experiments have been performed on different magnetic materials containing $3d$ transition elements. The differential methods of magnetic circular dichroism (MCD) and magnetic linear dichroism (MLD) have been applied to

some magnetic materials, particularly by Pisarev *et al.* (*131*). The structure and temperature dependence in MCD of the $^3A_2 \rightarrow {}^1F^2$ transition in $RbNiF_3$ has confirmed the magnetic structure (*159*). The origin of the $^3A_2 \rightarrow {}^1G^a$ transition of the Ni^{2+} ion in antiferromagnetic ($KNiF_3$) and ferrimagnetic ($RbNiF_3$) fluorides (*131*, *205*), which is characterized by a rather complex fine structure, can be ascribed to either spin orbit coupling with the nearest $^3T_1{}^a$ level (*57*) or exchange interaction between Ni^{2+} ions (*205*).

The far infrared spectra of $RbNiF_3$ have been interpreted on the basis of lattice vibrations of the different groups (*96*), and Raman diffusion studies have been made from 15 up to 300 K (*31*).

2. *Effects of Pressure on the Magnetic Properties of AMF_3 Phases*

Longo and Kafalas have shown that pressure favors the formation of structures containing the greatest number of compact cubic units (*86*, *104*, *105*). The transition sequence is, therefore, $2H \rightarrow 9R \rightarrow 4H$ (oxides) $\rightarrow 6H \rightarrow 3C$ (*84*) (Fig. 15). It is, thus, possible to transform a

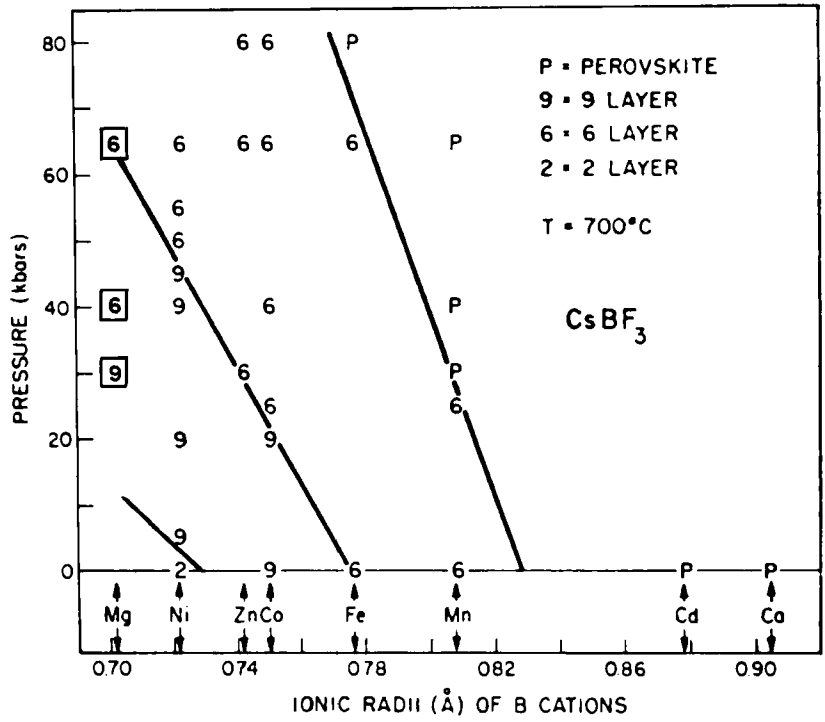

FIG. 15. Structural phase diagram of $CsM(II)F_3$ compounds. [From Longo and Kafalas (*104*), by permission of the *Journal of Solid State Chemistry*.]

TABLE VIII

MAGNETIC PROPERTIES OF THE AMF_3 POLYMORPHS[a]

Compound	Structure type			
	$BaNiO_3$ (2*L*)	$BaRuO_3$ (9*L*)	$BaTiO_3$ (6*L*)	Cubic perovskite (3*L*)
$CsMnF_3$		—	Antiferromagnetic T_N = 54 K (*102*)	[p = 26 kbar (*104*)]
$CsFeF_3$		—	Ferrimagnetic T_C = 60 K (*133*) T_C = 62 K (*51*)	[t = 500°C p = 70 kbar (*104*)]
$CsCoF_3$	—	Antiferromagnetic (*105*) T_N = 8 K θ_p = −62 K spin flop at 4.2 K at 11 kOe	(t = 700°C Ferrimagnetic p = 20 kbar) T_C = 50 K (*105*) θ_p = −65 K $\sigma_{s,0} = 0.8\,\mu_B$	—
$RbNiF_3$	—	—	Ferrimagnetic T_C = 139 K (*146*)	(p = 30 kbar) Antiferromagnetic T_N = 260 K (*86*)
$TlNiF_3$	—		Ferrimagnetic T_C = 150 K (*95*)	[p = 30 kbar (*169*)] Antiferromagnetic T_N = 240 K Weak ferromagnetism below 95 K
$CsNiF_3$	Monodimensional ferromagnetism below 80 K Antiferromagnetic order at T_N = 2.6 K θ_p = +8 K (*162*) θ_p = +22 K (*101*) θ_p = +30 K (*168*)	(p = 5 kbar) Paramagnetic down to 77 K θ = −75 K (*104*)	(p = 20 kbar) Ferrimagnetic T_C = 111 K $\sigma_{s,0} = 0.53\,\mu_B$ (*104*)	—

[a] Italic numbers in parentheses are reference citations.

fluoride showing monodimensional ferromagnetic ($CsNiF_3$) or antiferromagnetic properties ($CsCoF_3$) into a ferrimagnetic phase (*168*). In the same way, the ferrimagnetic fluorides $CsFeF_3$, $RbNiF_3$ (*86*), and $TlNiF_3$ (*169*) change under high pressures (20–50 kbar) into cubic perovskites, where the presence of 180° magnetic interactions M—F—M leads only to antiferromagnetic properties with a *G*-type magnetic structure (Table VIII). Figure 16 shows the various magnetic properties of $CsNiF_3$, which goes successively from the 2*H* variety through the 9*H* variety to the ferrimagnetic 6*H* polymorph (*168*). For $RbNiF_3$, the variation of the Curie temperature with pressure has been studied by Kafalas and Longo, who corroborate the prediction of Goodenough concerning the positive sign of $dT_c/dp = +0.60 \pm 0.2$ K/kbar for compounds with localized electrons (*65*).

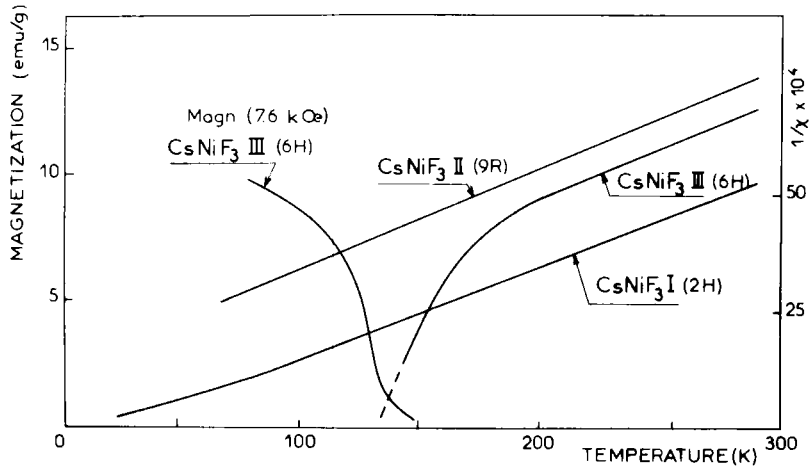

FIG. 16. Magnetic results of three polymorphs of $CsNiF_3$. [From Syono *et al.* (*168*), by permission of Centre National de la Recherche Scientifique.]

Longo *et al.* have also shown that $RbFeCl_3$, which has a 2*H* form at atmospheric pressure, is transformed into 9*R*, 6*H*, and 3*C* polymorph at 15, 20, and 35 kbar, respectively (*106*). The 6*H* form is ferrimagnetic ($T_c = 109$ K), and the saturation magnetization ($\sigma = 1.1\ \mu_B$) is in good agreement with the theoretical value.

3. *Ba_2NiTeO_6-Type (12R) Phases*

Recently, Dance *et al.* (*41*), by substituting the couple sodium-trivalent element in the $Cs_2NaM(III)F_6$ (*11*, *72*) [M(III) = 3*d* element] phases with a Ba_2NiTeO_6 structure (*94*) by two divalent elements

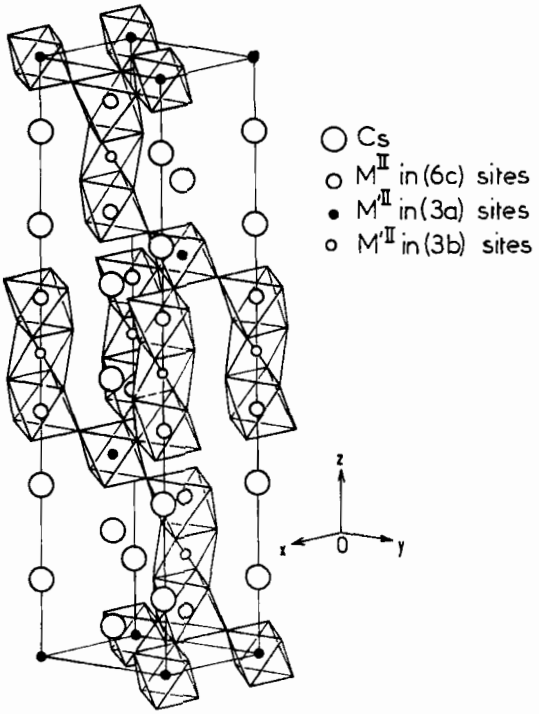

FIG. 17. The structure of $Cs_2M(II)M'(II)F_6$.

with sizes sufficiently different to favor an order, obtained the $Cs_2M(II)M'(II)F_6$ series [M(II) = Mn, Cd; M'(II) = Mg, Co, Ni, Zn]. When the 6*c*, 3*a*, and 3*b* sites of the 12*R* structure (Fig. 17) contain transition elements, these phases are ferrimagnetic (Cs_2MnCoF_6, Cs_2MnNiF_6) (Table IX). A general study of the 12*R* phases in the $CsMF_3$·$CsM'F_3$ system at different pressure has been considered (*42*).

TABLE IX

MAGNETIC DATA FOR 12*L* FERRIMAGNETIC FLUORIDES[a]

Compound	T_c (K)	$\sigma_{s,0}$ (μ_B)	$C_{exptl.}$	θ_p (K)
Cs_2MnCoF_6	53	1.99	8.19	−61
Cs_2MnNiF_6	61	2.40	5.96	−78

[a] From Dance *et al.* (*41*).

4. $Cs_4Mg_3F_{10}$-Type Phases

In 1970, Shafer *et al.* (*149*) studied the magnetic properties of $Cs_4M_3F_{10}$ compounds (M = Fe, Co, Ni), which are isostructural with $Cs_4Mg_3F_{10}$ (*9*, *164*). These phases, which present a complex magnetic behavior, have some structural features in common with the hexagonal phases previously studied. They are formed by three face-sharing octahedra units connected by a common corner. They form layers that are separated by the Cs^+ ions (Fig. 18). As in the 6*L* or 12*L* structures, the 90°, 180° superexchange and direct magnetic couplings are present. The magnetic orders observed involve interactions between the layers of $(M_3F_{10})_n^{4n-}$ units. These couplings are weak (interlayers M—M distances $\simeq$ 10 Å) and could explain the low values of the ordering temperatures (Table X). The large anisotropy observed on the crystals and the low values of magnetizations may be due to imperfect alignment of the moments.

The range of AMF_3 magnetic phases has been increased by reports of the existence of some cubic perovskites (with a Goldschmidt factor

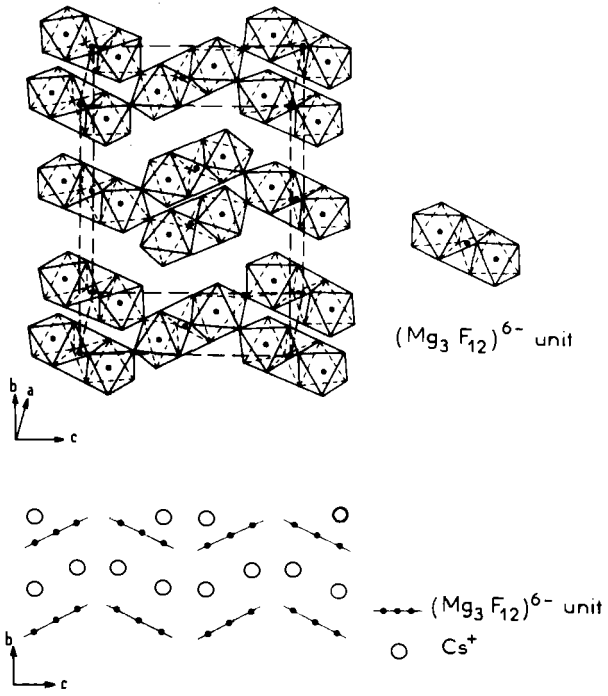

FIG. 18. The $Cs_4Mg_3F_{10}$-type structure.

TABLE X

MAGNETIC DATA FOR $Cs_4M_3F_{10}$ COMPOUNDS[a]

Compound	Transition temp. (K)	θ_p (K)	$\sigma_{s,0}$ (μ_B)
$Cs_4Fe_3F_{10}$	22	−36	—
$Cs_4Co_3F_{10}$	33	≃ −120	0.98
$Cs_4Ni_3F_{10}$	15	−106	0.06

[a] From Shafer *et al.* (*149*).

close to 1) presenting a succession of crystallographic transformations at low temperature, involving the presence of nonnegligible, spontaneous magnetizations: for $RbFeF_3$, $\sigma_0 \simeq 0.6\ \mu_B$ (*197*) and for $TlFeF_3$, $\sigma_0 \simeq 0.2\ \mu_B$ (*46*, *134*, *172*). Numerous structural, optical, and magneto-optical studies have been made on these phases (*30*, *171*, *192*).

D. CHIOLITE-TYPE COMPOUNDS

In 1958, Knox and Geller prepared $Na_5Fe_3F_{14}$ and reported on its likeness to natural chiolite $Na_5Al_3F_{14}$ (*92*). A precise structural determination of $Na_5Fe_3F_{14}$ was made finally in 1975 by Vlasse *et al.* (*183*). The similarity to chiolite has been confirmed, but the space groups are different [$P4/mnc$ for $Na_5Al_3F_{14}$ (*23*); $P4_22_12$ for γ-$Na_5Fe_3F_{14}$] and the octahedral environment of the iron atoms is quite distorted ($1.76 < Fe—F < 1.92$ Å).

The FeF_6 octahedra are connected to form layers with the formula $(Fe_3F_{14})_n^{5n-}$. The structure of each layer can be described as being built up of chains of octahedra bridged by one octahedron out of two (Fig. 19). One-third of the FeF_6 octahedra share four corners with their neighbors (2*a* sites), and two-thirds share two corners (4*d* sites). The sodium atoms are situated in the vacant sites in and between the layers. Table XI summarizes the crystallographic parameters of the $Na_5M_3F_{14}$ compounds.

Inside the layers the magnetic interactions result from nearly 180° superexchange couplings (Fig. 19b) via the fluorine *p* orbitals and are essentially antiferromagnetic. The difference of occupation by the iron atoms of the two sublattices (2*a* and 4*d*) leads to a spontaneous magnetization. The value of the magnetization expected is then,

$$\sigma_{s,0} = 2\mathbf{M}(4d) - \mathbf{M}(2a)$$

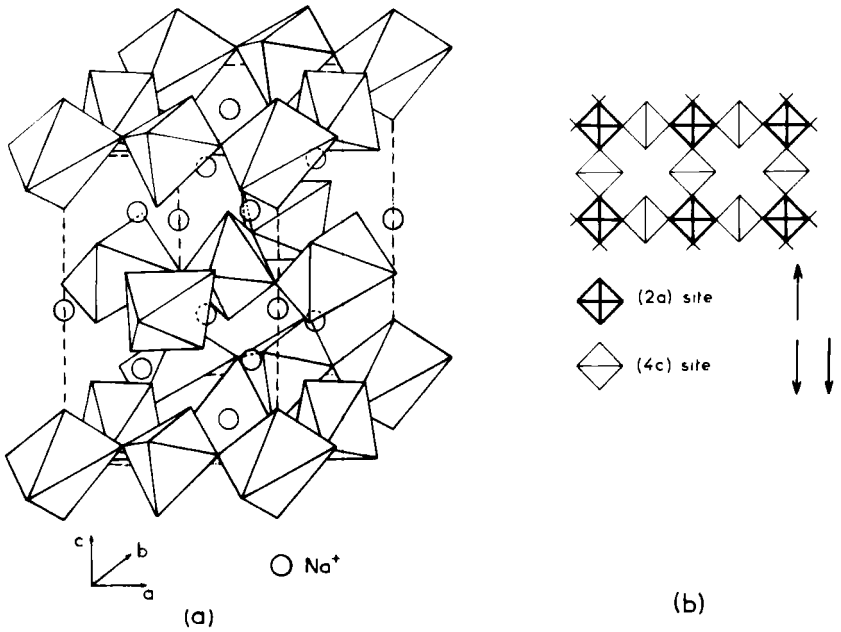

FIG. 19. (a) The structure of γ-$Na_5Fe_3F_{14}$ and (b) the schematization of a $(Fe_3F_{14})_n^{5n-}$ layer. [From Moriliere-Rioux (*116*).]

TABLE XI

CRYSTALLOGRAPHIC DATA FOR $Na_5M_3F_{14}$ PHASES

Compound	Cell parameters (Å) (tetragonal symmetry)		Color	Ref.
	a	*c*		
$Na_5Al_3F_{14}$	7.00	10.34	White	(*23*)
$Na_5Ti_3F_{14}$	7.48	10.30	Pink-gray	(*12*)
$Na_5V_3F_{14}$	7.33	10.36	Dark green	(*110*)
$Na_5Cr_3F_{14}$	7.32	10.34	Light green	(*113*)
γ-$Na_5Fe_3F_{14}$	7.345	10.40	Pink-beige	(*183*)
$Na_5Fe_2CoF_{14}$	7.33	10.34	Pink-beige	(*110*)
$Na_5Co_3F_{14}$	7.30	10.21	Light violet	(*110*)

The magnetic data (*93*, *110*) and the magnetic structure determination by Wintenberger *et al.* (*198*) showed that, in spite of the distance between two layers (5.2 Å), the net moments of each layer were aligned (parallel to *c*) leading to ferrimagnetism (Fig. 20). Table XII shows the magnetic parameters related to each transition element.

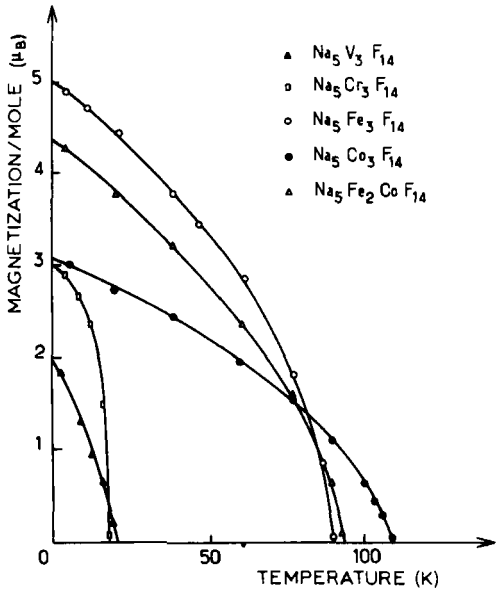

FIG. 20. Temperature dependence of the magnetization of $Na_5M_3F_{14}$ phases. [From Dance (*39*).]

The Curie temperatures of the vanadium and chromium compounds are particularly low because, in the case of V^{3+} and Cr^{3+} ions, only t_{2g}–$p\pi$–t_{2g} couplings are present. In the cases of Fe^{3+} and Co^{3+} e_g–$p\sigma$–e_g couplings are also present and are stronger because of greater orbital overlap. Moreover, the replacement of Fe^{3+} by Co^{3+} in chiolite increases the Curie temperature by 18 K. This result is a feature common to all the fluorinated compounds containing highspin Co^{3+} (*200*). It involves a strengthening of the M^{3+}—F—M^{3+} couplings due to an increase of the charge on the nucleus, leading to a decrease in the size of the M^{3+} ion and a tendency toward covalency. The transfer integral corresponding to the Co^{3+}—F bond becomes more important than for the Fe^{3+}—F bond and results in an increase of the exchange integral.

TABLE XII

MAGNETIC DATA FOR $Na_5M_3F_{14}$ PHASES

$Na_5M_3(III)F_{14}$ compounds	Ferrimagnetic region			Paramagnetic region			
	T_c (K)	$\sigma_{s,0}$ (exptl.) (μ_B mole^{-1})	$\sigma_{s,0}$ (theoret.) (μ_B mole^{-1})	θ_p (K)	C_M (exptl.)	C_M (theoret.) (spin-only values)	Ref.
$Na_5V_3F_{14}$	21	1.94	2	−48	2.44	3	(*110*)
$Na_5Cr_3F_{14}$	18	2.97	3	−32	5.44	5.61	(*113*)
$Na_5Fe_3F_{14}$	90	4.98	5	−95	11.55	13.14	(*110*)
$Na_5Fe_2CoF_{14}$	94	4.33	4.5 (random) 6 (ordered)	−100	10.53	11.76	(*110*)
$Na_5Co_3F_{14}$	108	3.10	4	−110	8.50	9	(*110*)

A Mössbauer study of $Na_5Fe_3F_{14}$ confirmed the ratio 1:2 between the 2*a* and the 4*d* sites occupied by the iron atoms (*183*) (Fig. 21). The sextuplet corresponding to the 2*a* sites can be deduced with high precision by supposing the main axis *z* of the electric field parallel to the hyperfine field, i.e., the *c* axis, confirming the flattening of the octahedron along this axis.

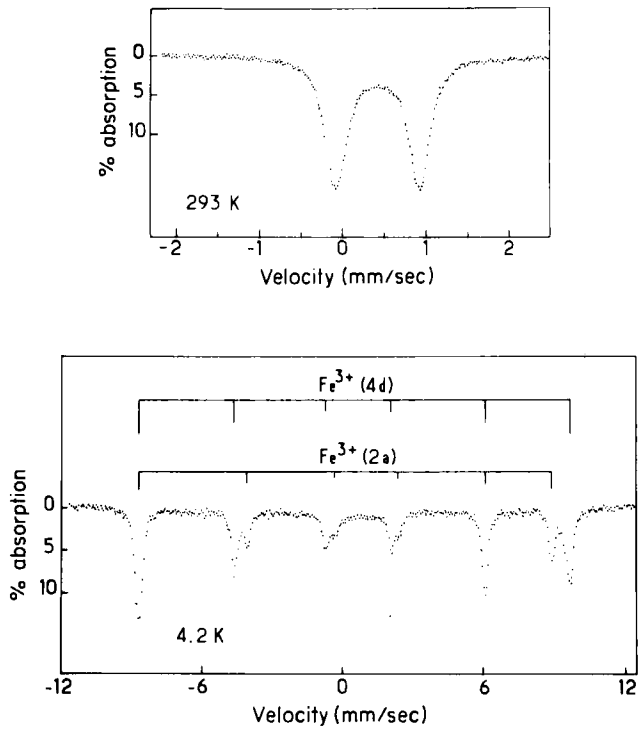

FIG. 21. Mössbauer spectra of γ-$Na_5Fe_3F_{14}$. [From Vlasse *et al.* (*183*) by permission of the *Journal of Solid State Chemistry*.]

Magnetic anisotropy measurements made on oriented single crystals corroborate the neutron diffraction data (*198*).

Ferrimagnetic resonance absorption of $Na_5Fe_3F_{14}$ has shown a large magnetic anisotropy field ($H_a \simeq 8000$ gauss at 65 K) (*160*). The absorption spectrum shows peaks at 15,000, 20,000, 26,000, and 29,500 cm^{-1} which correspond to transitions from the ground state $^6A_1(^6S_{5/2})$ to $^4T_1(^4\Gamma_4)$, $^4T_2(^4\Gamma_5)$, $^4A_1(^4\Gamma_2)$, and $^4E(^4\Gamma_1)$ and $^4T_2(^4\Gamma_5)$, respectively (Fig. 22).

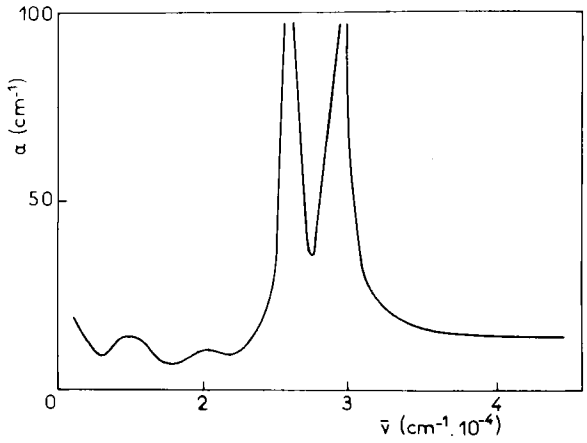

FIG. 22. Absorption spectrum of $Na_5Fe_3F_{14}$. [From Spencer *et al.* (*160*), by permission of *Physical Review Letters*.]

E. WEBERITE-TYPE COMPOUNDS

The structure of the weberite Na_2MgAlF_7 (*20*) has been determined by Byström (orthorhombic symmetry, space group *Imm2*) (*27*). The divalent and trivalent cations are located in fluorine octahedra and occupy, respectively, the 4*c* and 4*d* sites (average distances, Mg—F = 1.94 Å and Al—F = 1.83 Å). The $M(II)F_6$ octahedra share their six corners with their neighbors, whereas the $M(IV)F_6$ octahedra only share four of them. Their arrangement forms a three-dimensional network with the $M(II)M(III)F_7$ formula (Fig. 23). Table XIII summarizes the crystallographic parameters of some phases with the weberite structure.

This structure has many features in common with the hexagonal form of the tungsten bronzes and with the pyrochlore structure (Fig. 24) (*35*, *184*). In the three lattices, the octahedra form layers that contain tunnels with hexagonal or triangular sections. In the hexagonal bronzes, these layers are directly connected to each other by corners, but in the weberite they are associated by $M(III)F_6$ octahedra sharing four of their corners (Fig. 24b) and the connecting octahedra share their six corners in the pyrochlore structure.

In the weberite structure, the sodium atoms are situated in the middle of the hexagonal sections of the layers (4*d* sites), with the coordination 6, and between the layers, with the coordination 4 + 4 (4*c* sites). This structure may also be described as formed by zig-zag chains of $M(II)F_6$

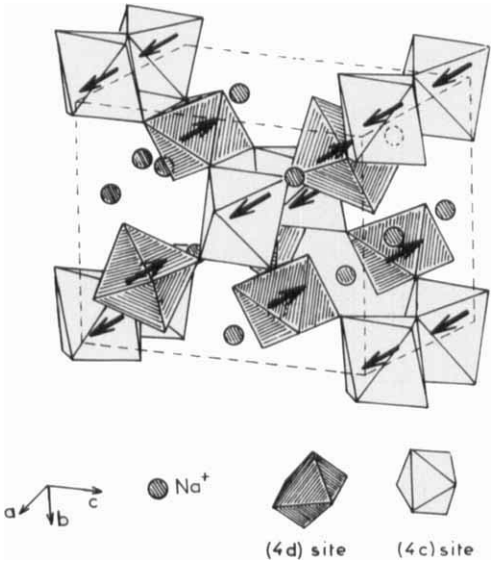

FIG. 23. The weberite structure.

TABLE XIII

CRYSTALLOGRAPHIC DATA FOR WEBERITE COMPOUNDS

Compound	Cell parameters (Å) (orthorhombic symmetry)			Color	Ref.
	a	*b*	*c*		
Na_2MgAlF_7 weberite	7.29	7.05	9.97	White	(*27*)
Na_2MgFeF_7	7.49	7.25	10.26	White	(*29*)
Na_2MnFeF_7	7.44	7.33	10.52	Beige	(*35*)
Na_2FeFeF_7	7.48	7.31	10.385	Brown	(*35*)
Na_2CoCrF_7	7.31	7.32	10.51	Green	(*78*)
Na_2CoFeF_7	7.405	7.325	10.405	Pink	(*35*)
Na_2NiAlF_7	7.31	7.07	10.04	Green	(*177*)
Na_2NiCrF_7	7.40	7.20	10.22	Green	(*78*)
Na_2NiFeF_7	7.46	7.23	10.32	Green	(*35*)
Na_2NiCoF_7	7.40	7.20	10.24	Light brown	(*35*)
Ag_2NiCrF_7	7.673	7.305	10.285	Green	(*40*)
Ag_2NiFeF_7	7.69	7.345	10.345	Yellow	(*40*)

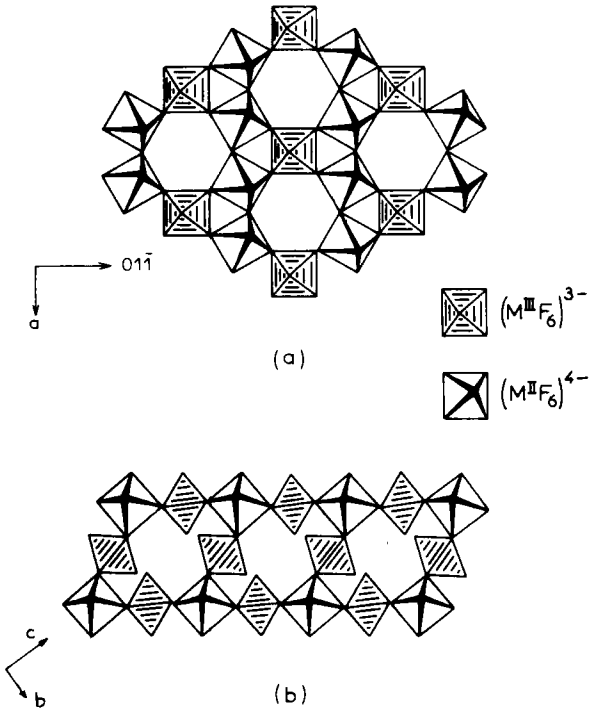

FIG. 24. (a) Idealized projection of the weberite structure on the (011) plane; (b) connection of the layers by $[M(II)F_6]^{3-}$ octahedra. [From Dance (*39*).]

octahedra sharing opposite corners connected by the $M(III)F_6$ octahedra (Fig. 24a).

Tressaud *et al.* (*177*) explained the diversity of the magnetic properties by considering the interactions involved. If the divalent element is diamagnetic, octahedra containing the M^{3+} ions are magnetically isolated (Fig. 24a) leading to the paramagnetism of Na_2MgFeF_7 for instance. When the trivalent element is diamagnetic (Al^{3+}, In^{3+}), the magnetic interactions only occur along the chains of $M(II)F_6$ octahedra connected by two opposite corners, and the materials are antiferromagnetic (e_g–$p\sigma$–e_g and t_{2g}–$p\pi$–t_{2g} type). This is the case, for instance, with Na_2FeAlF_7, Na_2NiAlF_7, Ag_2NiAlF_7, and Ag_2NiInF_7, which are antiferromagnetic. A neutron diffraction study has shown that in Na_2NiAlF_7 the 143° Ni—F—Ni couplings were antiferromagnetic below 14 K (*80*) and that the spins that lie in the a–b plane are not collinear and form a 40° angle with the a axis. This canting is responsible for the spontaneous magnetization in the $A_2M(II)AlF_7$ phases

TABLE XIV

MAGNETIC DATA FOR FERRIMAGNETIC WEBERITES

$Na_2M(II)M(III)F_7$ compounds	Ferrimagnetic region			Paramagnetic region			
	T_c (K)	$\sigma_{s,0}$ (exptl.) (μ_B mole^{-1})	$\sigma_{s,0}$ (theoret.) (μ_B mole^{-1})	θ_p (K)	C_M (exptl.)	C_M (theoret.) (spin-only values)	Ref.
Na_2MnFeF_7	$T_N = 97$[a]	0.14[b]	—	−134	8.19	8.76	(*177*)
Na_2FeFeF_7	84	0.75	1	−104	7.42	7.38	(*177*)
Na_2CoFeF_7	80	1.2	2	−100	7.35	6.26	(*177*)
Na_2NiCrF_7	4	—[c]	1	−35	2.90	2.87	(*112*)
Na_2NiFeF_7	90	1.5	3	−50	4.60	5.38	(*35*)
Na_2NiFeF_7	90	2.3 (Single crystal)	3				(*39*)
Na_2NiCoF_7	126	0.9	2	−88	4.27	4	(*177*)
Ag_2NiCrF_7	10	—[c]	1	−28	3.08	2.87	(*177*)
Ag_2NiFeF_7	103	2.1	3	−61	4.51	5.38	(*177*)

[a] Antiferromagnetic by compensation.
[b] Ferromagnetic component.
[c] Impossible to be determined accurately.

(*80, 175*). When both the divalent and trivalent ions are paramagnetic, two types of interactions are present: a superexchange coupling between two divalent ions within a chain and a superexchange interaction between a divalent and a trivalent element. Heger and Viebahn-Hänsler determined the magnetic structure of Na_2NiFeF_7 and showed that the spins lie along the a axis (Fig. 23) (*79*). The ferrimagnetism is due to strong negative interactions between Ni^{2+} and Fe^{3+} ions (Ni—F—Fe angle = 142°) which align ferromagnetically the spins of the Ni^{2+} ions. A magnetic study on single crystals has also confirmed the orientation of the spins. The magnetization (observed 2.3 μ_B) along the easy axis is in good agreement with the calculated value.

Table XIV gives the magnetic data for the ferrimagnetic weberites. In the case of A_2NiCrF_7 compounds, an interpretation of the type as discussed in the foregoing cannot be given because no negative interaction can occur between Ni^{2+} and Cr^{3+} (d^8 and d^3 configuration). As Na_2NiCrF_7 and Ag_2NiCrF_7 are not ferromagnetic (*40*), a different magnetic structure must be present. The (σ, T) curves of Na_2FeFeF_7, Na_2CoFeF_7, and Na_2NiCoF_7 display a deviation around 20 K (Fig. 25): The nonsaturation of one of the magnetic ions below T_c could explain the rapid increase of the magnetization at low temperature, but a nonlinear and complex arrangement between 20 K and T_c must also be considered. Compensation of the two magnetic sublattices in Na_2MnFeF_7

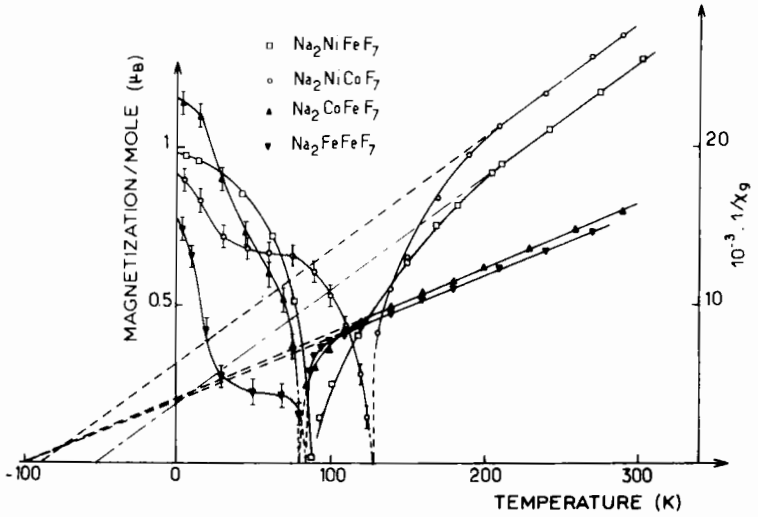

FIG. 25. Temperature dependence of the reciprocal susceptibility and magnetization of ferrimagnetic weberites. [From Dance (*39*).]

(d^5–d^5) leads to an antiferromagnetic compound. A spontaneous magnetization appears below T_N and is comparable with the values obtained for $RbFeF_3$ and $TlFeF_3$ (*134*). In the series $Na_2NiM(III)F_7$, for the same divalent ion, the Curie temperatures increase with the sequence Cr^{3+}, Fe^{3+}, Co^{3+}. This has already been observed with the chiolite fluorides (*110*). On the contrary, the divalent element has only a weak influence on the order temperatures [$Na_2M(II)Fe(III)F_7$ series] (Table XIV). The increase of the Curie temperatures when sodium is replaced by silver has been explained by examining the nature of the A(I)—F bonding (*40*).

Magnetic anisotropy measurements have confirmed the direction of the spins in Na_2NiFeF_7 (*39*).

F. M(II)M′(III)F_5-Type Compounds

During the last 10 years, a large number of fluorides with the general formula $M(II)M'(III)F_5$ have been investigated (*48*, *185*). When the trivalent ions M′ correspond to aluminum, 3*d* transition elements, or gallium, these phases were found to exist if the radius of the divalent ion M was larger than approximately 0.8 Å.* A structural classification based on the size of the M(II) ion and the ratio $r_{M(II)}/r_{M'(III)}$ has been established by Von der Mühll and Ravez (*186*). In discussing magnetic materials, this section only deals with compounds where the M(II) and M′(III) radii are relatively close.

These fluorides are known to crystallize in at least five related structures (*38*): monoclinic (*C*/2*c*) Cr_2F_5 (*163*, *166*); orthorhombic (*Ama* 2) $MnAlF_5$ (*36*, *136*); monoclinic (*C*2/*c*) $CaCrF_5$ (*49*, *88*); monoclinic ($P2_1/c$) $CaFeF_5$ (*186*); and monoclinic (*C*2/*c*) (*45*) $MnCrF_5$ (*55*). A common feature of all these structures is parallel $[M'(III)F_5]^{2-}$ chains of trans corner-shared octahedra containing the M′(III) ions, these chains being held together by the M(II) cations. In $MnAlF_5$ and Cr_2F_5, the M(II) cations occupy chains of edge-shared octahedra parallel to the $M'(III)F_5$ chains as illustrated in Fig. 26. The monoclinic Cr_2F_5 structure may be derived from the orthorhombic $MnAlF_5$ structure by a cooperative Jahn–Teller distortion of the edge-shared Cr(II) octahedra, which produces the usual two long Cr(II)—F bonds along one axis and four short bonds in a plane nearly perpendicular (tilted 18° in Cr_2F_5) to this axis. In $CaCrF_5$, $CaFeF_5$, and $MnCrF_5$, the calcium atoms are also situated between four $M(III)F_5$ files but are surrounded by rather distorted polyhedra that form chains along the *c* axis.

* The values of the ionic radii have been taken from Shannon and Prewitt (*152*).

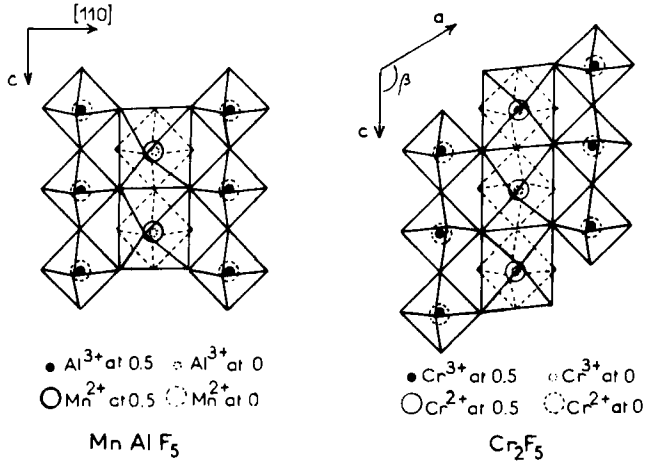

FIG. 26. Structures of $MnAlF_5$ and Cr_2F_5.

1. *$MnAlF_5$-Type Ferrimagnetic Solid Solution*

In $MnAlF_5$, isolated chains of edge-shared octahedra contain Mn(II) cations (Fig. 27) and the compound is paramagnetic at 4 K (*174*). This observation is consistent with weak, ferromagnetic Mn—Mn pair interactions along the *c* axis in the Mn-doped ZnF_2, which has the rutile structure (*26*, *124*). This weak interaction appears to reflect an almost perfect cancellation of two moderate contributions to the Mn(II)—Mn(II) interactions: antiferromagnetic delocalization superexchange ($Mn^{2+} + Mn^{2+} \rightleftharpoons Mn^{3+} + Mn^{+}$) and ferromagnetic correlation superexchange (covalent spin polarization of $p\sigma$ and $p\sigma'$ orbitals

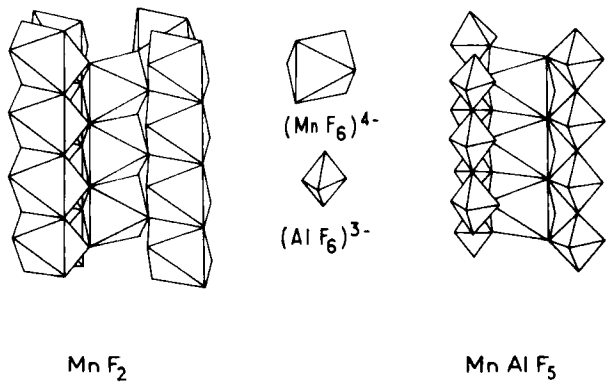

FIG. 27. A comparison of $MnAlF_5$ and rutile structures.

at the fluorine) (*67*). In $MnAlF_5$, the Weiss constant is slightly negative: $\theta_p = -6$ K. A neutron diffraction study has shown the compound to be antiferromagnetic below 2.4 K (*197*).

Ferrimagnetic solid solutions with the formula $MnAl_{1-x}M_x(III)F_5$ [M(III) = 3*d* transition element] can be obtained, particularly in the system $MnAl_{1-x}Fe_xF_5$ ($0 < x \leq 0.58$) (*174*). Here the 180° Fe(III)—F—Fe(III) interactions should be antiferromagnetic and strong [$T_N = 363$ K in FeF_3 (*193*)], but the weaker antiferromagnetic ~125° Mn(II)—F—Fe(III) interactions are in competition. Initial Fe substitutions introduce ferrimagnetic clusters consisting of an Fe(III) ion moment oriented antiparallel to the nearest-neighbor Mn(II) ion moments. If Fe(III) ions are next-nearest neighbors in a $[M(III)F_5]^{2-}$ string, a larger ferrimagnetic cluster may be formed. However, if Fe(III) ions are nearest neighbors in a string, then the Fe(III)—F—Fe(III) interactions compete with the Mn(II)—F—Fe(III) interactions, and the magnetic order within a cluster is more complex. When the Fe atom concentration is just large enough to introduce long-range magnetic order, ferrimagnetic clusters are coupled with complex magnetic clusters. As the Fe atom concentration increases, the complex clusters probably interact to form a multimagnetic phase system consisting of antiferromagnetic and ferrimagnetic regions. The hypothetical antiferromagnetic phase $MnFeF_5$ would certainly be a spiral-spin configuration. Figure 28a shows the increase of the Curie temperatures with x, and Fig. 28b the variation of the extrapolated (σ, $1/H$) magnetization with x.

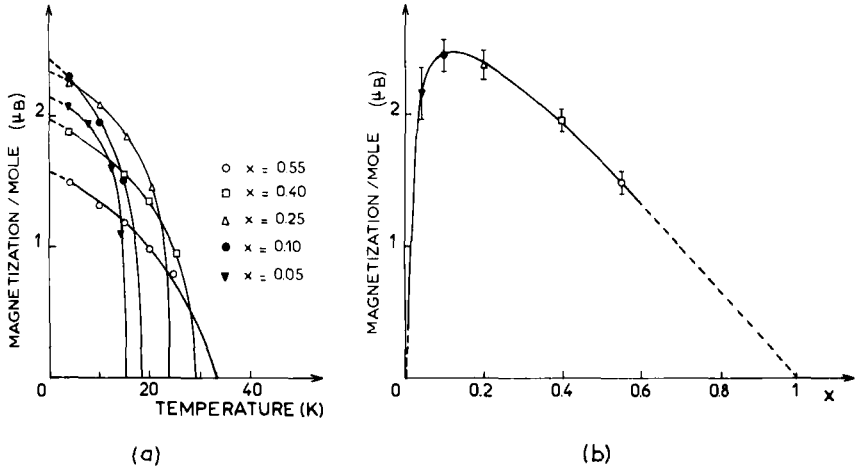

FIG. 28. Variation of the magnetization of $MnAl_{1-x}Fe_xF_5$ series (a) with temperature and (b) with x.

2. Cr_2F_5-Type Compounds

While he was studying the system CrF_2—CrF_3, Sturm (*166*) isolated a phase with a composition near to Cr_2F_5. It existed over the compositional range $Cr_2F_{4.8}$–$Cr_2F_{4.9}$, corresponding to a mean chromium valence of 2.4 to 2.45. The structure determined by Steinfink and Burns (*163*) corresponds to the ideal composition Cr_2F_5. Tressaud *et al.* isolated $Cr(II)M(III)F_5$ compounds for M = Al, Ti, V in the same range of composition (*175*). For M = Mn, Fe, Co, the oxidation reduction reaction ($CrF_2 + MF_3 \rightarrow CrF_3 + MF_2$) prohibited the formation of $CrMF_5$ phases.

Table XV summarizes the lattice parameters for the $CrMF_5$ compounds, and Table XVI gives the magnetic data together with a spin-only, molar, Curie constant calculated for the composition formula $Cr_{1.2}M_{0.8}F_{4.8}$. Figure 29 shows, in the case of ferrimagnetic $CrTiF_5$ and $CrVF_5$, the reciprocal molar susceptibilities vs. temperature and the magnetization σ_s (in Bohr magnetons per mole) below the Curie temperatures, T_c = 26 and 40 K, respectively.

Osmond (*123*) had predicted an antiferromagnetic order in Cr_2F_5. This prediction was confirmed by magnetic measurements (*175*), but

TABLE XV

LATTICE PARAMETERS FOR THE $Cr(II)M(III)F_5$ COMPOUNDS[a]

Parameter	$CrAlF_5$	$CrTiF_5$	$CrVF_5$	Cr_2F_5
a (Å)	7.58 ± 0.01	7.98 ± 0.01	7.91 ± 0.01	7.77 ± 0.005
b (Å)	7.46 ± 0.01	7.65 ± 0.01	7.60 ± 0.01	7.54 ± 0.005
c (Å)	7.25 ± 0.01	7.70 ± 0.01	7.63 ± 0.01	7.44 ± 0.005
β (°)	123.7 ± 0.2	125.2 ± 0.2	125.0 ± 0.2	124.25 ± 0.1

[a] From Tressaud *et al.* (*175*).

TABLE XVI

MAGNETIC DATA FOR THE $Cr(II)M(III)F_5$ COMPOUNDS[a,b]

Composition		T_N (K)	T_c (K)	θ_p (K)	$\sigma_{s,0}$ (μ_B)	C_M (exptl.)	C_M (calc.)
$CrAlF_5$	P	—	—	−3 ± 2	—	2.57 ± 0.03	2.55
$CrTiF_5$	F	—	26 ± 3	−78 ± 5	1.78 ± 0.10	3.59 ± 0.03	3.88
$CrVF_5$	F	—	40 ± 3	−51 ± 5	0.86 ± 0.10	4.02 ± 0.03	4.40
$CrCrF_5$	AF	40 ± 3	—	−95 ± 5	—	4.98 ± 0.03	5.08

[a] From Tressaud *et al.* (*175*).

[b] P, paramagnetic; F, ferromagnetic; AF, antiferromagnetic.

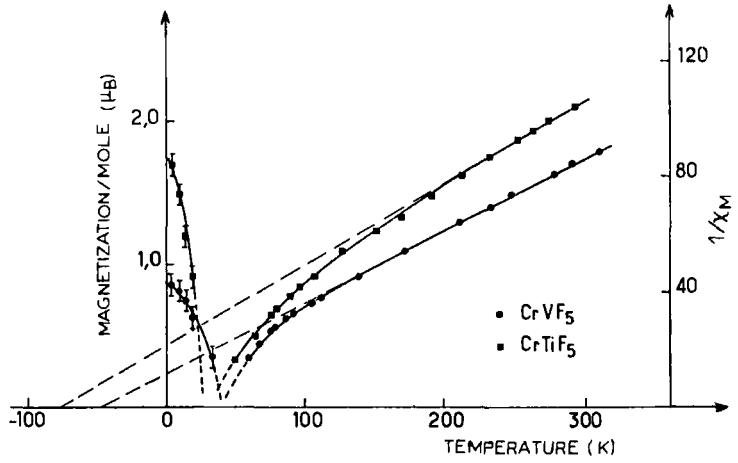

FIG. 29. Temperature dependence of the reciprocal susceptibility and magnetization of $CrTiF_5$ and $CrVF_5$. [From Dance (*39*).]

because of the single-ion anisotropy, it anticipates in addition an antiferromagnetic spin canting. Antiferromagnetic coupling between corner and face-center-like strings in the (001) plane guarantees antiferromagnetism, even though the individual *c* axis strings may carry a ferromagnetic component.

Goodenough explained the ferrimagnetic properties of $CrTiF_5$ and $CrVF_5$ by the competition between interatomic exchange interactions (*175*). In $CrTiF_5$, the Cr(II)—F—Ti(III) interactions are dominated by electron transfer from half-filled *d* orbitals on Cr(II) ions to empty *d* orbitals on Ti(III) ions which are ferromagnetic. On the other hand, couplings between two Ti(III) ions (d^1–d^1) are antiferromagnetic due to the preferential occupancy of the d_{xy} orbital by the unique electron. Since magnetic anisotropy is expected to stabilize the Ti(III) ion moments close to the *c* axis, the energy of the competitive interactions can be minimized by a ferromagnetic component along the *b* axis and antiferromagnetic components along the *c* axis for both Ti(III) ion and Cr(III) ion chains. In $CrVF_5$, the V(III) ion having two outer *d* electrons, a spin orbit coupling associated with the $^3T_{1g}(d^2)$ configuration at octahedral site must introduce a strong spin lattice coupling below the magnetic ordering temperature (*66*). The signs of the interactions in $CrVF_5$ are similar to those predicted for $CrTiF_5$; however, the strong magnetic anisotropy associated with the V(III) ion inhibits a large canting of the moments away from the *b* axis. With such a model

for the ferrimagnetism of $CrTiF_5$ and $CrVF_5$, magnetic saturation (assuming fixed cant angles) of a polycrystalline sample requires rotation of the ferromagnetic component against the crystalline anisotropy. From this analysis, this anisotropy should be much larger for $CrVF_5$, as observed experimentally.

G. Miscellaneous

Finally, it must be reported that many fluorides, without being ferrimagnetic, show spontaneous magnetization below the magnetic ordering temperature (*34*). A substantial number of structures are liable to show spontaneous magnetism: for instance, chain structures [$BaFeF_5$ (*62*)], phases containing the same ion in two different oxidation states [$K_{0.5}VF_3$ (*37*)], rutile-type phases [NiF_2 (*74, 111, 117*)] perovskite-related structures [MF_3, AMF_3], and ferromagnetic compounds with a K_2NiF_4 structure [A_2CuF_4; A = K, Rb, Cs (*42a, 81, 98, 201*)].

Among the 3*d* transition element trifluorides, for instance, neutron diffraction studies (*200*) have shown that CrF_3, FeF_3, and CoF_3 presented a *G* magnetic structure. In the last two, $e_g - p\sigma - e_g$ superexchange interactions are present and lead to high Néel temperatures of 363 K (*103, 150, 176*) and 460 K, respectively (*200*). Weak ferromagnetism appears below T_N and, thus, is present at room temperature ($\sigma_s \simeq 0.01\ \mu_B$ at 293 K). The magnetic moment of FeF_3 was found to lie in the plane perpendicular to the rhombohedral axis (*193, 196*). A great deal of work has been done on microwave resonance, optical, and magneto-optical properties of this material for applications in optical communications (modulators, rotators, beam deflectors) and storage or display devices (memory systems, holograms, magnetic bubbles propagation) (*99, 139, 151, 195, 199*). Compound CrF_3 also presents magnetization ($\sigma = 0.04\ \mu_B$) below $T_N = 80$ K (*76, 77*).

We have already reported the existence of magnetism in AMF_3 perovskites with a Goldschmidt factor close to 1 ($RbFeF_3$, $TlFeF_3$). Similarly, when the tolerance factor is small (lower than 0.8), fluorides crystallize with the $GdFeO_3$ structure (*21, 138, 180*). These *G*-type antiferromagnetic phases have been widely studied (*59, 122, 134, 203*) and present below T_N weak ferromagnetism of the Dzialoshinski type (*50*). Moriya reported that this behavior was due to deviations from an uniaxial alignment of antiparallel spins (i.e., canting of the sublattices) and to two physical interactions: single-ion magnetocrystalline anisotropy and antisymmetric exchange interaction (*118*); Epstein *et al.* showed that the second type of interaction was responsible for the weak ferromagnetism in $NaNiF_3$ (*54*).

As a final example of the potential interaction of fluorinated compounds we may consider Pd_2F_6, from which Bartlett *et al.* have obtained, by extrapolation of the $1/\chi$ curve, a positive Curie temperature (*13*, *14*). The recent data on absolute molar saturation magnetization ($\sigma = 1.76\ \mu_B$) and a neutron diffraction study in progress (*179*) will give much information on this new type of ferromagnetic fluoride.

ACKNOWLEDGMENTS

The authors wish to thank Prof. P. Hagenmuller and Dr. J. Portier for the constant interest they took in this work, Profs. H. J. Emeléus and A. G. Sharpe for their help in the realization of this article, and Profs. N. Bartlett and J. B. Goodenough for helpful discussions. They wish also to thank the Fluorine Research Group in Bordeaux, especially Dr. J. Grannec and L. Lozano.

REFERENCES

1. Aleonard, R., Barbier, J. C., and Pauthenet, R., *C. R. Hebd. Seances Acad. Sci.* **242**, 2531 (1956).
2. Als-Nielsen, J., Birgeneau, R. J., and Guggenheim, H. J., *Phys. Rev. B* **6**, 2030 (1972).
3. Anderson, P. W., *Phys. Rev.* **79**, 350 (1950); **79**, 705 (1950); **115**, 2, (1959).
4. Anderson, P. W., *in* "Magnetism" (G. T. Rado and H. Suhl, eds.), Vol. 1, p. 1. Academic Press, New York, 1964.
5. Anderson, P. W., *Solid State Phys.* **14**, 99 (1963).
6. Arnott, R. J., and Longo, J. M., *J. Solid State Chem.* **2**, 416 (1970).
7. Babel, D., *Z. Naturforsch. A* **20**, 165 (1965).
8. Babel, D., "Structure and Bonding," Vol. 3. Springer-Verlag, Berlin and New York, 1967.
9. Babel, D., *Z. Anorg. Allg. Chem.* **369**, 117 (1969).
10. Babel, D., *J. Solid State Chem.* **2**, 582 (1970).
11. Babel, D., Haegele R., Pausewang, G., and Wall F., *Mater. Res. Bull.* **8**, 1371 (1973).
11a. Babel, D., and Verscharen, W., unpublished results.
12. Barbalat, C., and Vedrine, A., *Rev. Chim. Miner.* **11**, 388 (1974).
13. Bartlett, N., and Quail, J. W., *J. Chem. Soc.* p. 3728 (1961).
14. Bartlett, N., and Rao, P. R., *Proc. Chem. Soc.* p. 393 (1964).
15. Bartlett, N., *in* "Preparative Inorganic Reactions" (W. J. Jolly, ed.), Vol. 2, p. 301. Wiley (Interscience), New York, 1965.
16. Bertaut, E. F., and Forrat, F., *C. R. Hebd. Seances Acad. Sci.* **242**, 382 (1956).
17. Bertaut, E. F., and Pauthenet, R., *Proc. Inst. Electr. Eng. Part B* **104**, 261 (1957).
18. Boky, L. P., Syrnikov, P. P., Yudin, V. M., and Smolensky, G. A., *Solid State Commun.* **5**, 927 (1967).
19. Bougon, R., Ehretsmann, J., Portier, J., and Tressaud, A., *in* "Preparative Methods in Solid State Chemistry" (P. Hagenmuller, ed.) p. 401. Academic Press, New York, 1972.
20. Bovgad, R., *Medd. Groenl.* **119**, 107 (1938).
21. Bozorth R. M., *Phys. Rev. Lett.* **1**, 362 (1958).
22. Bradley, R. S., ed., *Advan. High Pressure Res.*, **1**–**4** (1966–1970).

23. Brosset, C., *Z. Anorg. Allg. Chem.* **238**, 201 (1938).
24. Brown, H. A., and Luttinger, J. M., *Phys. Rev.* **100**, 685 (1955).
25. Burbank, R. D., and Evans, H. T., *Acta Crystallogr.* **1**, 330 (1948).
26. Butler, M., Jaccarino, V., Kaplan, N., and Guggenheim, H. J., *Phys. Rev. B* **1**, 3058 (1970).
27. Byström, A., *Ark. Kemi B* **18**, 1 (1944).
28. Chamberland, B. L., U.S. Patent 316, 355 (1966).
29. Chassaing, J., *C. R. Hebd. Seances Acad. Sci. Ser. C* **268**, 2188 (1969).
30. Chen, F. S., Guggenheim, H. J., Levinstein, H. J., and Singh, S., *Phys. Rev. Lett.* **19**, 948 (1967).
31. Chinn, B. R., and Zeiger, H. J., *Phys. Rev. Lett.* **21**, 1589 (1968).
32. Claverie, J., Ph.D. Thesis, Univ. of Bordeaux, 1972.
33. Claverie, J., Portier, J., and Hagenmuller, P., *Z. Anorg. Allg. Chem.* **393**, 314 (1972).
34. Conolly, T. F., and Copenhaver, E. D., "Bibliography of Magnetic Materials and Tabulation of Magnetic Transition Temperatures." Plenum, New York, 1972.
35. Cosier, R., Wise, A., Tressaud, A., Grannec, J., Olazcuaga, R., and J. Portier, *C. R. Hebd. Seances Acad. Sci.* **271**, 142 (1970).
36. Cousseins, J. C., Erb, A. and Freundlich, W., *C. R. Hebd. Seances Acad. Sci* **268**, 717 (1969).
36a. Cros, C., Dance, J. M., Grenier, J. C., Wanklyn, B. M., and Garrard, B. J., *Mater. Res. Bull.* (to be published).
37. Cros, C., Feurer, R., Grenier, J. C., Pouchard, M., and Hagenmuller, P., *Mater. Res. Bull* **11**, 539 (1976).
38. Dance, J. M., and Tressaud, A., *C. R. Hebd. Seances Acad. Sci.* **277**, 379 (1973).
39. Dance, J. M., Ph.D. Thesis, Univ. of Bordeaux, 1974.
40. Dance, J. M., Grannec, J., Jacoboni, C., and Tressaud, A., *C. R. Hebd. Seances Acad. Sci.* **279**, 601 (1974).
41. Dance, J. M., Grannec, J., and Tressaud, A., *C. R. Hebd. Seances Acad. Sci.* **281**, 91 (1975).
42. Dance, J. M., unpublished work, 1975.
42a. Dance, J. M., Grannec, J., and Tressaud, A. *C. R. Hebd. Seances Acad. Sci.* **283**, 115 (1976).
43. Danielian, A., and Stevens, K. W. H., *Proc. Phys. Soc.* **77**, 124 (1961).
44. de Pape, R., Portier, J., Gauthier, G., and Hagenmuller, P., *C. R. Hebd. Seances Acad. Sci.* **265**, 1244 (1967).
45. de Pape R., Ferey, G., Poulain, M., Grandjean, D., and Hardy, A., *Acta Crystallogr. Sect. B* (to be published).
46. Dillon, J. F., and Guggenheim, H. J., U.S. Patent 3, 609, 008 (1971).
47. Donohue, P. C., Katz, L., and Ward, R., *Inorg. Chem.* **4**, 306 (1965).
48. Dumora, D., Ravez, J., and Hagenmuller, P., *Bull. Soc. Chim. Fr.* **6**, 2010 (1971).
49. Dumora, D., Von der Mühll, R., and Ravez, J., *Mater. Res. Bull.* **6**, 561 (1971).
50. Dzialoshinsky, I., *Soviet Phys.—JETP* **5**, 1259 (1957); *J. Phys. Chem. Solids* **4**, 241 (1958).
51. Eibschütz, M., Holmes, L., Guggenheim, H. J., and Levinstein H. J., *J. Appl. Phys.* **40**, 1312 (1969).
52. Elbinger, G., Jäger, E., Keilig, W., and Perthel, R., *J. Phys. (Colloq. C,)* **32**, 626 (1971).
53. Elbinger, G., Funke, A., Kieinert, P., Rosemann, P., and Keilig, W., *Z. Anorg. Allg. Chem.* **393**, 193 (1972).
54. Epstein, A., Makovsky, J., Melamud, M., and Shaked, H., *Phys. Rev.* **174**, 560 (1968).

55. Ferey, G., Leblanc, M., Jacoboni, C., and de Pape R., *C. R. Hebd. Seances Acad. Sci.* **273**, 700 (1971).
56. Francillon, M., Loriers, J., and Villers G., *C. R. Hebd. Seances Acad. Sci.* **266**, 1372 (1968).
57. Ferguson, J., Guggenheim, H. J., and Wood, D. L., *J. Chem. Phys.* **40**, 822 (1964).
58. Frei, E., and Schieber, M., U.S. Patent 207, 021 (1962).
59. Friedmann, M., Melamud, M., Makovsky, J., and Shaked, H., *Phys. Rev. B* **3** (1), 129 (1970).
60. Garrard, B. J., Wanklyn, B. M., and Smith, S. H., *J. Cryst. Growth* **22**, 169 (1974).
61. Garton, G. and Wanklyn, B. M., *J. Cryst. Growth* **1**, 19 (1967).
62. Georges, R., Ravez, J., Olazcuaga, R. and Hagenmuller, P., *J. Solid State Chem.* **9**, 1 (1974).
63. Goodenough, J. B., *Phys. Rev.* **100**, 564 (1955).
64. Goodenough, J. B., "Magnetism and the Chemical Bond." Wiley, New York, 1963.
65. Goodenough, J. B., *Phys. Rev.* **164**, 785 (1967).
66. Goodenough, J. B., *Phys. Rev.* **171**, 466 (1968).
67. Goodenough, J. B., *Proc. Winter School Solid State Chem.*, 1974.
68. Gorter, E. W., *Philips Res. Rep.* **9**, 321, 403 (1954).
69. Grannec, J., Ph.D. Thesis, Univ. of Bordeaux, 1970.
70. Grannec, J., Lozano, L., Portier, J., and Hagenmuller, P., *Z. Anorg. Allg. Chem.* **385**, 26 (1971).
71. Grannec, J., unpublished work (1974).
72. Grannec, J., Sorbe, P., Portier, J., and Hagenmuller, P., *C. R. Hebd. Seances Acad. Sci.* **280**, 45 (1975).
73. Guggenheim, H. J., *J. Appl. Phys.* **34**, 2482 (1963).
74. Haefner, K., and Dachs, H., *J. Chem. Phys.* **43**, 2910 (1965).
75. Hall, T., *Rev. Sci. Instrum.* **31**, 125 (1960).
76. Hansen, W. N., and Griffel, M., *J. Chem. Phys.* **28**, 902 (1958).
77. Hansen, W. N., *J. Appl. Phys.* **30**, 3045 (1959).
78. Hänsler, R., and Rüdorff, W., *Z. Naturforsch. B* **25**, 1306 (1970).
79. Heger, G., and Viebahn-Hänsler, R., *Solid State Commun.* **11**, 1119 (1972).
80. Heger, G., *Int. J. Magn.* **5**, 119 (1973).
80a. Herpin, A. "Theorie du Magnetisme." Presses Univ. France, Paris, 1968.
81. Hirakawa, K., and Ikeda, H., *J. Phys. Soc. Jpn.* **33**, 1483 (1972); **35**, 1329 (1973).
82. Hoy, G. R., and Chandra, S., *J. Chem. Phys.* **47**, 961 (1967).
83. Ichinose, N., and Kurihara, K., *J. Phys. Soc. Jpn.* **20**, 1530 (1965).
84. Ikeda, T., Nakaue, A., and Inoue, K., *Mater. Res. Bull.* **9**, 1371 (1974).
85. Jäger, E., *Phys. Status Solidi* **51**, 713 (1972); **52**, 61 (1972).
86. Kafalas, J. A., and Longo, J. M., *Mater. Res. Bull.* **3**, 501 (1968); *J. Appl. Phys.* **40**, 1601 (1969).
87. Kanamori, J., *J. Phys. Chem. Solids* **10**, 87 (1959).
88. Kang Kun Wu and Brown, I. D., *Mater. Res. Bull.* **8**, 593 (1973).
89. Katz, L., and Ward, R., *Inorg. Chem.* **3**, 205 (1964).
90. Kestigian, M., Leipziger, F. D., Croft, W. J., and Guidoboni, R., *Inorg. Chem.* **5**, 1462 (1966).
91. Kirk, R. E., and Othmer, D. F., "Encyclopedia of Chemical Technology" Vol. 9. Wiley, New York, 1966.
91a. Kittel, C., "Introduction to Solid State Physics." Wiley, New York, 1971.
92. Knox, K., and Geller, S., *Phys. Rev.* **110**, 771 (1958).
93. Knox, K., U.S. Patent, 2, 945, 744 (1960).

94. Köhl, P., Müller, U., and Reinen, D., *Z. Anorg. Allg. Chem.* **392**, 124 (1972).
95. Kohn, K., Fukuda, R., and Iida, S., *J. Phys. Soc. Jpn.* **22**, 333 (1967).
96. Kohn, K., and Nakagawa, I., *Bull. Chem. Soc. Jpn.* **43**, 3780 (1970).
97. Kramers, H. A., *Physica* **1**, 182 (1934).
98. Kubo, H., Shimohigashi, K., and Yamada, I., *J. Phys. Soc. Jpn.* **34**, 1687 (1973).
99. Kurtzig, A. J., and Guggenheim, H. J., *Appl. Phys. Lett.* **16**, 43 (1970).
100. Lander, J. J., *Acta Crystallogr.* **4**, 148 (1951).
101. Lebesque, J. V., Snel, J., and Smit, J. J., *Solid State Commun.* **13**, 371 (1973).
102. Lee, K., Portis, A. M., and Witt, G. L., *Phys. Rev.* **132**, 144 (1963).
103. Levinson, L. M., *J. Phys. Chem. Solids* **29**, 1331 (1968).
104. Longo, J. M., and Kafalas, J. A., *J. Solid State Chem.* **1**, 103 (1969).
105. Longo, J. M., Kafalas, J. A., O'Connor, J. R., and Goodenough, J. B., *J. Appl. Phys.* **41**, 935 (1970).
106. Longo, J. M., Kafalas, J. A., Menyuk, N., and Dwight, K., *J. Appl. Phys.* **42**, 1561 (1971).
106a. Mabbs, F. E., and Machin, D. J., "Magnetism and Transition Metal Complexes." Chapman & Hall, London, 1973.
107. McGuire, T. R., and Shafer, M. W., *J. Appl. Phys.* **39**, 1130 (1968).
108. McGuire, T. R., Moruzzi, V. L., and Shafer, M. W., *J. Appl. Phys.* **41**, 956 (1970).
109. McGuire, T. R., and Shafer, M. W., *J. Phys.* (*Colloq.* 2-3) **32**, 627 (1971).
110. McKinzie, H., Dance, J. M., Tressaud, A., Portier, J., and Hagenmuller, P., *Mater. Res. Bull.* **7**, 673 (1972).
111. Matarrese, L. M., and Stout, J. W., *Phys. Rev.* **94**, 1792 (1954).
111a. Menil, F., Steger, J., and Dance, J. M., *J. Phys. Chem. Solids* (to be published).
112. Miranday, J. P., 3rd cycle Thesis, Univ. of Caen, France, 1972.
113. Miranday, J. P., Ferey, G., Jacoboni, C., Dance, J. M., Tressaud, A., and de Pape, R., *Rev. Chim. Miner.* **12**, 187 (1975).
114. Morell, A., Ph.D. Thesis, Univ. of Bordeaux, 1973.
115. Morell, A., Tanguy, B., Portier, J., Hagenmuller, P., and Nicolas, J., *J. Fluorine Chem.* **3**, 351 (1974).
116. Moriliere-Rioux, C., 3rd cycle Thesis, Univ. of Bordeaux, 1974.
117. Moriya, T., *Phys. Rev.* **117**, 635 (1960).
118. Moriya, T., *Phys. Rev.* **120**, 91 (1960); *in* "Magnetism" (G. T. Rado and H. Suhl, eds.), Vol. 1. Academic Press, New York, 1964.
119. Néel, L., *Ann. Phys.* **18**, 5 (1932); **5**, 232 (1936); **3**, *137* (1948).
120. Néel, L., Pauthenet, R., Rimet, G., and Giron, V. S., *J. Appl. Phys.* **31**, 27 (1960).
121. Nouet, J., Jacoboni, C., Ferey, G., Gerard, J. Y., and de Pape, R., *J. Cryst. Growth* **8**, 94 (1971).
122. Ogawa, S., *J. Phys. Soc. Jpn.* **15**, 2361 (1960).
123. Osmond, W. P., *Proc. Phys. Soc. London* **87**, 767 (1966).
124. Owen, J., Brown, M. R., Coles, B. A., and Stevensen, R. W. H., *J. Phys. Soc. Jpn.* **17**, Suppl. BI, 428 (1962).
125. Owen, J., and Thornley, J. H. M., *Rep. Prog. Phys.* **29**, 675 (1966).
126. Pauthenet, R., *C. R. Hebd. Seances Acad. Sci.* **243**, 1499 (1956).
127. Pauthenet, R., *Ann. Phys.* **3**, 424 (1958).
128. Peacock, R. D., *Prog. Inorg. Chem.* **2**, p. 193. Interscience, New York (1960).
128a. Pebler, J., Schmidt, K., Babel, D., and Verscharen, W., *Z. Natur. forsch. B* (to be published).
129. Pickart, S. J., Alperin, H. A., and Nathans, R., *J. Phys.* **25**, 565 (1964).
130. Pickart, S. J., and Alperin, H. A., *J. Appl. Phys.* **39**, 1332 (1968); **42**, 1617 (1971).

131. Pisarev, R. V., Siny, I. G., and Smolensky, G. A., *Solid State Commun.* **5**, 959 (1967).
132. Pisarev, R. V., Siny, I. G., and Smolensky, G. A., *Fiz. Tverd. Tela (Leningrad)* **9**, 3149 (1967).
133. Portier, J., Tressaud, A., Pauthenet, R., and Hagenmuller, P., *C. R. Hebd. Seances Acad. Sci.* **267**, 1329 (1968).
134. Portier, J., Tressaud, A., Dupin, J. L., and Hagenmuller, P., *Mater. Res. Bull.* **4**, 45 (1969).
135. Portier, J., Tanguy, B., Morell, A., Pauthenet, R., Olazcuaga, R., and Hagenmuller, P., *C. R. Hebd. Seances Acad. Sci.* **270**, 821 (1970).
135a. Rado, G. T., and Suhl, H., eds., "Magnetism: A Treatise on Modern Theory and Materials," Vols. I, II, and III. Academic Press, New York, 1963–1965.
136. Rimsky, A., Thoret, J., and Freundlich, W., *C. R. Hebd. Seances Acad. Sci.* **270**, 407 (1970).
137. Robbins, M., Lerner, S., and Banks, E., *J. Phys. Chem. Solids* **24**, 759 (1963).
138. Robbins, M., Pierce, R. D., and Wolfe, R., *J. Phys. Chem. Solids* **32**, 1789 (1971).
139. Rossol, F. C., Le Craw, R. C., Guggenheim, H. J., and Tabor, W. J., *Phys. Lett. A* **28**, 689 (1969).
140. Rüdorff, W., and Kändler, J., *Naturwissenschaften* **49**, 230 (1962).
141. Rüdorff, W., Kändler, J., and Babel, D., *Z. Anorg. Allg. Chem.* **317**, 261 (1962).
142. Rüdorff, W., Lincke, G., and Babel, D., *Z. Anorg. Allg. Chem.* **320**, 150 (1963).
143. Rüshbrooke, G. S., and Wood, P. J., *Mol. Phys.* **1**, 257 (1958).
144. Schieber, M. M., "Experimental Magnetochemistry." North-Holland Publ., Amsterdam, 1967.
145. Schmitz-Dumont, O., and Bornefeld, H., *Z. Anorg. Allg. Chem.* **287**, 120 (1956).
146. Shafer, M. W., McGuire, T. R., Argyle, B. E., and Fan, G. J., *Appl. Phys. Lett.* **10**, 202 (1967).
147. Shafer, M. W., and McGuire, T. R., *Proc. Meeting Electrochem. Soc., Boston, 133rd, 1968.*
148. Shafer, M. W., and McGuire, T. R., *J. Phys. Chem. Solids* **30**, 1989 (1969).
149. Shafer, M. W., McGuire, T. R., and Weidenborner, J. E., *J. Appl. Phys.* **42**, 1489 (1971).
150. Shane, J. R., Kedzie, R. W., Kestigian, M., Lyons, D. H., and Wang, F. F. Y., Air Force Cambridge Res. Lab. Rep. Contract no AF 19 (628), p. 5128 (1966).
151. Shane, J. R., and Kestigian, M., *J. Appl. Phys.* **39**, 1027 (1968).
152. Shannon, R. D., and Prewitt, C. T., *Acta Crystallogr. Sect. B* **25**, 925 (1969).
153. Sharpe, A. G., *Advan. Fluorine Chem.* 1, 29 (1959).
154. Simanov, Y. P., Batsanova, L. R., and Korba, L. M., *Zh. Neorg. Khim.* **2**, 2410 (1957).
155. Smart, J. S., *J. Phys. Chem. Solids* **11**, 97 (1959).
156. Smart, J. S., *in* "Magnetism" (G. T. Rado and H. Suhl, eds.), Vol. III, p. 63. Academic Press, New York, 1963.
157. Smit, J., and Wijn, H. P. J., "Ferrites." Wiley, New York, 1959.
158. Smolensky, G. A., Yudin, V. M., Syrnikov, P. P., and Sherman, A. B., *JETP Lett. Engl. Transl.* **8**, 2368 (1967).
159. Smolensky, G. A., Pisarev, R. V., Petrov, M. A., Moskalev, V. V., Siny, I. G., and Yudin, V. M., *J. Appl. Phys.* **39**, 568 (1968).
160. Spencer, E. G., Berger, S. B., Linares, R. C., and Lenzo, P. V., *Phys. Rev. Lett.* **10**, 236 (1963).
161. Stanley, H. E., and Kaplan, T. A., *Phys. Rev. Lett.* **17**, 913 (1963).
162. Steiner, M., Krüger, W., and Babel, D., *Solid State Commun.* **9**, 227, (1971).
163. Steinfink, H., and Burns, J. H., *Acta Crystallogr.* **17**, 823 (1964).

164. Steinfink, H., and Brunton, G., *Inorg. Chem.* **8**, 1665 (1969).
165. Stemple, N. R., and Wnuck, R. C. (1968), cited in Weidenborner and Bednowitz (*188*).
166. Sturm, B. J., *Inorg. Chem.* **1**, 665 (1962).
167. Suits, J. C., McGuire, T. R., and Shafer, M. W., *Appl. Phys. Lett.* **12**, 406 (1968).
168. Syono, Y., Akimoto, S., and Kohn, K., *Colloq. Int. CNRS* **188**, 415 (1970).
169. Syono, Y., Akimoto, S., and Kohn, K., *J. Phys. Soc. Jpn.* **26**, (4), 903 (1969).
170. Tanguy, B., Portier, J., Morell, A., Olazcuagua, R., Francillon, M., Pauthenet, R., and Hagenmuller, P., *Mater. Res. Bull.* **6**, 63 (1971).
171. Testardi, L. R., Levinstein, H. J., and Guggenheim, H. J., *Phys. Rev. Lett.* **19**, 503 (1967).
172. Tressaud, A., de Pape, R., Portier, J., and Hagenmuller, P., *C. R. Hebd. Seances Acad. Sci., Paris* **266**, 984 (1968).
173. Tressaud, A., Menil, F., Georges R., Portier, J., and Hagenmuller, P., *Mater. Res. Bull.* **7**, 1339 (1972).
174. Tressaud, A., Parenteau, J. M., Dance, J. M., Portier, J., and Hagenmuller, P., *Mater. Res. Bull.* **8**, 565 (1973).
175. Tressaud, A., Dance, J. M., Ravez, J., Portier, J., Hagenmuller, P., and Goodenough, J. B., *Mater. Res. Bull.* **8**, 1467 (1973).
176. Tressaud, A., Dance, J. M., Menil, F., Portier, J., and Hagenmuller, P., *Z. Anorg. Allg. Chem.* **399**, 231 (1973).
177. Tressaud, A, Dance, J. M., Portier, J., and Hagenmuller, P., *Mater. Res. Bull.* **9**, 1219 (1974).
178. Tressaud, A., Dance, J. M., Parenteau, J. M., Launay, J. C., Portier, J., and Hagenmuller, P., *J. Cryst. Growth*, **32**, 221 (1976).
179. Tressaud, A., Wintenberger, M., Bartlett, N., and Hagenmuller, P., *C. R. Hebd. Seances Acad. Sci.* **282**, 1069 (1976).
180. Treves, D., *Phys. Rev.* **125**, 1843 (1962); *J. Appl. Phys.* **36**, 1033 (1965).
181. Van Vleck, J. H., *Rev. Mod. Phys.* **17**, 27, 1945; **25**, 220 (1953).
182. Van Vleck, J. H., *J. Phys. Radium* **12**, 262 (1951).
183. Vlasse, M., Menil, F., Moriliere, C., Dance, J. M., Tressaud, A., and Portier, J., *J. Solid State. Chem.*, **17**, 291 (1976).
184. Vlasse, M., Chaminade, J. P., Massies, J. C., and Pouchard, M., *J. Solid State Chem.* **12**, 102 (1975).
185. Von der Mühll, R., Andersson, S., and Galy, *J., Acta Crystallogr., Sect. B* **27**, 2345 (1971).
186. Von der Mühll, R., and Ravez, J., *Rev. Chim. Miner.* **11**, 652 (1974).
187. Wang, F. Y., and Kestigian, M., *J. Appl. Phys.* **37**, 975 (1966).
188. Weidenborner, J. E., and Bednowitz, A. L., *Acta Crystallogr., Sect. B* **26**, 1464 (1970).
189. Weiss, P. R., *Phys. Rev.* **74**, 1493 (1948).
190. Wells, A. F., "Structural Inorganic Chemistry," Vol. 2, p. 390, 3rd ed. Oxford Univ. Press (Clarendon), London and New York, 1962.
191. Went, J. J., Rathenau, G. W., Gorter, E. W., and Van Oosterhout, G. W., *Philips Tech. Rev.* **13**, 194 (1952).
192. Wertheim, G. K., Guggenheim, H. J., Williams, H. J., and Buchanan, D. N. E., *Phys. Rev.* **158**, 446 (1967).
193. Wertheim, G. K., Guggenheim, H. J., and Buchanan, D. N. E., *Solid State Commun.* **5**, 537 (1967).
194. Wertheim, G. K., Guggenheim, H. J., Williams, H. J., and Buchanan, D. N. E., *J. Appl. Phys.* **39**, 1253 (1968).

195. Wertheim, G. K., Guggenheim, H. J., and Buchanan, D. N. E., *Phys. Rev.* **169**, 465 (1968).
196. Wertheim, G. K., Guggenheim, H. J., and Buchanan, D. N. E., *Phys. Rev. B* **2**, 1392 (1970).
197. Wintenberger, M., Dance, J. M., and Tressaud, A., *Solid State Commun.* **17**, 185 (1975).
198. Wintenberger, M., Dance, J. M., and Tressaud, A., *Solid State Commun.*, **17**, 1355 (1976).
199. Wolfe, R., Kurtzig, A. J., and Le Craw, R. C., *J. Appl. Phys.* **41**, 1218 (1970).
200. Wollan, E. O., Child, H. R., Koeler, W. C., and Wilkinson, M. K., *Phys. Rev. B* **112**, 1132 (1958).
201. Yamada, I., *J. Phys. Soc. Jpn.* **28**, 1585 (1970); **33**, 979 (1972).
202. Yamaguchi, Y., and Sakuraba, T., *J. Phys. Soc. Jpn.* **38**, 1011 (1975).
203. Yudin, V. M., and Sherman, A. B., *Phys. Status Solidi* **20**, 759 (1967).
204. Zalkin, A., Lee, K., and Templeton, D. H., *J. Chem. Phys.* **37**, 697 (1962).
205. Zammarchi, G., and Bongers, P. E., *Solid State Commun.* **6**, 27 (1968).

Note Added in Proof

A recent neutron diffraction study has shown that in Cs_2MnNiF_6 the Mn atoms are in fact located in the 3*a* sites and in half of the 6*c* sites (Fig. 17) and the Ni atoms are in the 3*b* sites and in the remaining half of the 6*c* sites (*42*).

Single crystals of light green $K_5V_3F_{14}$ with the chiolite structure have been grown. A magnetic study has shown ferrimagnetic properties below T_C = 18 K [$\sigma_{s,0}$(exptl.) = 2.1 μ_B] (*36a*).

A new refinement of the weberite structure performed on Na_2NiFeF_7 confirmed the *Imm2* space group; however Na_2MnFeF_7 has been shown to derive from the weberite structure by a different connection of the layers shown in Fig. 24 (*11a*). Na_2MFeF_7 compounds have also been studied by Mössbauer spectroscopy (*111a*, *128a*).